

University of South Bohemia

Faculty of Science

Study of Babesia microti acquisition by ticks

Master thesis

Bc. Pavla Šnebergerová

Supervisor: RNDr. Marie Jalovecká, Ph.D.

Co-supervisor: RNDr. Veronika Urbanová, Ph.D.

České Budějovice 2019

Šnebergerová P, 2019, Study of *Babesia microti* acquisition by ticks Mgr Thesis, in English – p. 59, Faculty of Science, University of South Bohemia, České Budějovice, Czech Republic.

Annotation

Acquisition of the apicomplexan parasite *Babesia microti* by the tick host has not been intensively investigated so far. To address this circumstance, AMA-1 (Apical membrane antigen-1) known to participate in host cell invasion, and sexual stage-specific protein CCp2 were selected as potential markers of *B. microti* developmental stages inside the tick host. In line with previous research, AMA-1 has been validated by indirect immunofluorescence as a specific antigen of *B. microti* invasive stages in vertebrate host blood. In addition, the immunogenic potential of this protein was confirmed. Despite the *ama-1* gene expression was examined in tick organs, AMA-1 protein was not detected in parasite stages – presumably kinetes – observed in epithelial cells of the tick gut wall. Therefore, AMA-1 protein does not appear to be a suitable universal marker of *B. microti* invasive stages in the tick. The *ccp2* gene expression was confirmed also in the tick tissues and indicates the presence of the sexual stages in the gut lumen. Yet, the specificity of CCp2 protein as a marker for *B. microti* sexual stages needs to be further investigated.

Financial support

This work was supported by the “Centre for research of pathogenicity and virulence of parasites” (no. CZ.02.1.01/0.0/0.0/16_019/0000759) funded by European Regional Development Fund (ERDF) and Ministry of Education, Youth and Sport (MEYS).

I hereby declare that I worked on this master thesis on my own and used only the resources mentioned in the bibliography.

I hereby declare that, in accordance with Article 47b of Act No. 111/1998 in the valid wording, I agree with the publication of my master thesis, in full to be kept in the Faculty of Science archive, in electronic form in publicly accessible part of the STAG database operated by the University of South Bohemia in České Budějovice accessible through its web pages.

Further, I agree to the electronic publication of the comments of my supervisor and thesis opponents and the record of the proceedings and results of the thesis defense in accordance with aforementioned Act No. 111/1998. I also agree to the comparison of the text of my thesis with the Theses.cz thesis database operated by the National Registry of University Theses and a plagiarism detection system.

Date.....

Signature.....

Acknowledgements

In the first place, I wish to thank Dr. Petr Kopáček for the opportunity to become a member of his research team and to participate in the research in his laboratory. I would like to express my deep gratitude to my supervisor Dr. Marie Jalovecká; for her patient guidance, useful critiques of this research work and for her positive energy when we tackled obstacles. I would also like to thank Dr. Veronika Urbanová; for the assistance with microscopy analysis. I would like to extend my thanks to all members of the research team of Dr. Kopáček and Dr. Ondřej Hajdušek; for their assistance during experiments and for making friendly work atmosphere. Finally, the biggest thank goes to my parents who were supporting and encouraging me throughout my studies.

Table of contents

1. Introduction	1
1.1. <i>Babesia</i> genus.....	1
1.1.1. Bovine and canine babesiosis.....	2
1.1.2. Human babesiosis	3
1.2. <i>Babesia microti</i>	4
1.2.1. Natural hosts of <i>Babesia microti</i>	4
1.2.2. Life cycle of <i>Babesia microti</i>	5
1.2.3. Apical complex	8
1.3. Apical membrane antigen 1 (AMA-1)	9
1.3.1. Structure of AMA-1	9
1.3.2. Role of AMA-1 in host cell invasion	9
1.3.3. AMA-1 in the lifecycle of apicomplexans	10
1.4. CCp2.....	11
2. Objectives	13
3. Material and Methods	14
3.1. Parasite and laboratory animals	14
3.2. Propagation of <i>B. microti</i> in BALB/c mice	14
3.3. Determination of parasitemia of <i>B. microti</i> in murine blood	15
3.4. Tick maintenance and feeding set up	15
3.5. DNA extraction	16
3.6. RNA extraction and cDNA synthesis.....	17
3.7. PCR and gel electrophoresis.....	18
3.8. Quantitative PCR	20
3.8.1. Absolute and relative quantification	20
3.9. Cloning of <i>ama-1</i> and <i>ccp2</i> genes.....	20
3.10. Expression and purification of AMA-1 and CCp2 recombinant proteins.....	22
3.11. Protein refolding	23
3.12. Rabbit immunization and preparation of polyclonal antibodies.....	23
3.13. Reducing SDS PAGE and Western blot.....	23
3.14. Preparation of the blood samples and tick gut samples for immunolocalization of <i>B. microti</i>	24
3.15. Repeated infections of mice with <i>B. microti</i>	24
4. Results	26
4.1. <i>B. microti</i> infection in mice and growth curve monitoring	26
4.2. Absolute quantification of <i>B. microti</i> in the gut and salivary glands of the ticks	27

4.3. Relative expression of <i>ama-1</i> gene.....	29
4.3.1. Relative expression of <i>ama-1</i> gene in the murine blood positive for <i>B. microti</i>	29
4.3.2. Relative expression of <i>ama-1</i> gene in the gut and salivary glands of ticks feeding on mice in different phases of parasite growth curve.	30
4.4. AMA-1 recombinant protein synthesis and antisera production	33
4.5. Anti-AMA-1 antibodies detected <i>B. microti</i> in the murine blood.....	35
4.6. Immunodetection of <i>B. microti</i> in the gut of fully fed nymph.....	36
4.7. Evaluation of immunogenicity of <i>B. microti</i> AMA-1 protein in BALB/c mice.....	37
4.7.1. Primary infection protects mice against re-infection with <i>B. microti</i>	37
4.7.2. Infected mice generate antibodies targeting AMA-1 protein.....	39
4.8. Relative expression of <i>ccp2</i> gene.....	40
4.8.1. Relative expression of <i>ccp2</i> gene in the murine blood infected with <i>B. microti</i>	40
4.8.2. Relative expression of <i>ccp2</i> in the gut and salivary glands of ticks feeding on mice with different level of parasitemia.....	41
4.9. Expression and purification of CCp2 recombinant protein.....	43
5. Discussion.....	45
6. Conclusion.....	51
7. References	52

1. Introduction

1.1. *Babesia* genus

The members of the *Babesia* genus are tick-transmitted intraerythrocytic unicellular organisms. They are classified to the phylum Apicomplexa together with widely known species of *Plasmodium*, *Cryptosporidium* and *Toxoplasma* genera (Votykka et al. 2017). Genus *Babesia* comprises of numerous species which cluster four clades of total ten within the order Piroplasmida (Fig. 1). *Babesia* parasites can be found worldwide since their presence depends on the distribution of their hosts i. e. ticks and vertebrates. They infect a broad range of wild as well as domestic animals. Humans are rather accidental hosts, although the incidence of human babesiosis rises worldwide (Yabsley and Shock 2013, Vannier et al. 2015). *Babesia* species have become both financial and public health threat worldwide (Homer et al. 2000; Irwin 2009; Gohil et al. 2013).

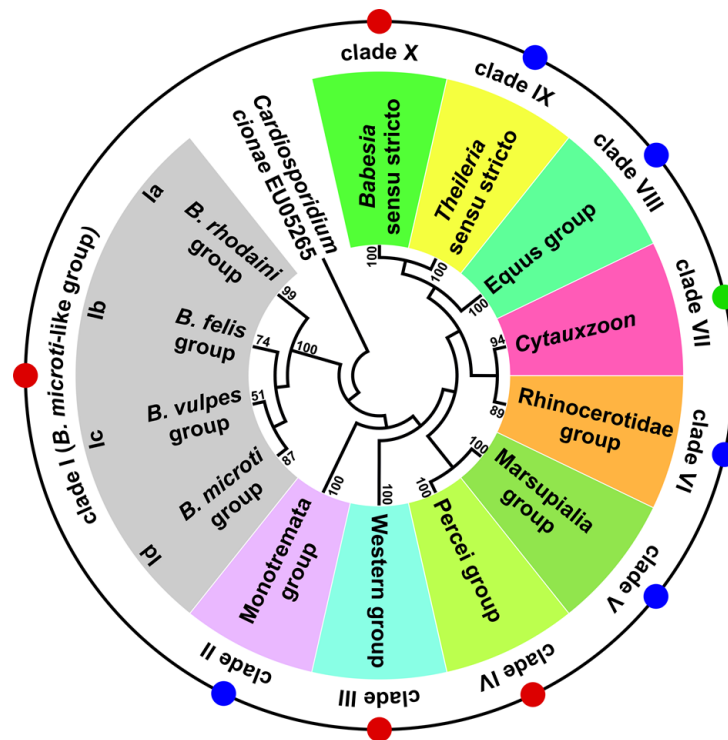


Figure 1: Molecular phylogeny of the order Piroplasmida. Piroplasmids comprise at least ten principal lineages of which *Babesia* constitute four clades i. e. *Babesia sensu stricto* and three lineages collectively referred to as *Babesia sensu lato* – Percei, Western, and *B. microti*-like groups. Red, blue and green dots represent clades comprising piroplasmids referred to as *Babesia*, *Theileria* and *Cytauxzoon* species, respectively (Jalovecka et al. 2019).

1.1.1. Bovine and canine babesiosis

The major impact of *Babesia* parasites occurs in the livestock industry. Specifically, *Babesia bovis* and *Babesia bigemina*, transmitted in tropical and subtropical regions, and *Babesia divergens*, found in northern and western Europe, are the main causative agents of bovine babesiosis (Bock et al. 2004; Gohil et al. 2010). The infection is manifested by intravascular hemolysis and anemia. However, it can progress more severely and it may result in multi-organ failure (Gohil et al. 2013; Suarez et al. 2019). Vaccination appears to be a more promising and feasible tool to control bovine babesiosis in comparison to available chemotherapeutics (de Waal and Combrink 2006). Nowadays, the emphasis is put on the development of affordable recombinant vaccine without side effects (Gohil et al. 2013).

One of the target hosts of *Babesia* species are also canines. Canine babesiosis is caused by numerous species worldwide. In some areas, their distribution interferes (Irwin 2009). For example *Babesia canis*, *Babesia vogeli*, newly characterized *Babesia vulpes* (Baneth et al. 2015) and *Babesia gibsoni* infect dogs in Europe (Solano-Gallego and Baneth 2011). Highly virulent *Babesia rossi* is the causative agent of canine babesiosis in Africa (Oyamada et al. 2005). Additionally, *B. gibsoni*, previously referred to as an Asian-type, is distributed also in the USA (Birkenheuer et al. 2005) and Australia (Jefferies et al. 2007). Severity of canine babesiosis ranges from subclinical infection to widespread organ failure (Solano-Gallego and Baneth 2011).

At the present time, no options for effective control of infections caused by members of *Babesia* genus are available. Despite the constant research on understanding mechanisms of transmission and pathophysiology of *Babesia* parasites as well as on immune mechanisms ongoing in the hosts, the treatment and prevention still remain limited (Irwin 2009; Gohil et al. 2013).

1.1.2. Human babesiosis

Human babesiosis is an emerging zoonotic disease which is caused by several species of *Babesia* genus. The first case of the human infection in Europe was documented in former Yugoslavia (Skrabalo and Deanovic 1957). The parasite has been classified as *B. divergens*, the common agent of bovine disease, which is nowadays the most prevalent causative agent of human babesiosis in Europe (Zintl et al. 2003). The areas with more than half of reported cases of human babesiosis in Europe are France and British Isles (Hildebrandt et al. 2013). The evidence of the infections has been kept also in other countries e.g. Finland (Haapasalo et al. 2010), Germany (Haselbarth et al. 2007), Poland (Welc-Faleciak et al. 2010), Portugal (Centeno-Lima et al. 2003), etc. *Babesia venatorum*, a deer species originally characterized as *B. divergens*, was documented to cause moderately-severely manifested infections of patients in Austria, Germany, and Italy (Herwaldt et al. 2003; Haselbarth et al. 2007). Documented cases of infections with *B. divergens* can be therefore inaccurate since both species were not distinguished from each other before.

Regarding the American continent and human babesiosis, the most prevalent agent causing the disease is a rodent species *Babesia microti* (Dammin et al. 1981). The parasite is transmitted by American tick species *Ixodes scapularis* (Yabsley and Shock 2013) or also via blood-transfusions (Leiby 2011). Geographical distribution of the parasite is concentrated in the Northeast and upper Midwest of the USA (Homer et al. 2000). According to epidemiological statistics of the Centre for Disease Control and Prevention from 2017, 1994 cases of human babesiosis were confirmed with the highest prevalence in New England region, specifically the state of Massachusetts, and Mid-Atlantic, namely the state of New York (excluding New York City) (CDC, Annual Tables of Infectious Disease Data, 2017). However, the statistics might be underestimated since the infection may be of mild symptoms or in some case asymptomatic. This fact is also supported by studies on *B. microti* seropositivity (Gray et al. 2010).

As *B. microti* was considered to be endemic species, there was no emphasis placed on medical awareness or diagnostic methods in Europe. Therefore, accurate epidemiology data of the disease is missing (Hildebrandt et al. 2013). Currently, there are several known strains of *B. microti* in Europe (Gray et al. 2010). There have been cases of *B. microti* infection verified in Poland (Welc-Faleciak et al. 2015) and Germany (Haselbarth et al. 2007). The analysis of seroprevalence confirmed infections with *B. microti* also in Switzerland (Foppa et al. 2002). With an increasing trend of traveling as well as with increasing number

of immunocompromised persons, infections with *B. microti* will probably rise in Europe in the future (Hildebrandt et al. 2013).

Outside the American continent and Europe, cases of human babesiosis are rare. Yet the infections with *B. microti* or *B. microti*-like parasites occurred in Australia (Senanayake, Paparini et al. 2012), Taiwan (Shih et al. 1997), Japan (Wei et al. 2001) and with KO1 novel *Babesia* spp. in Korea (Kim et al. 2007)

In immunocompetent individuals, infection is usually asymptomatic or it develops into a mild form of symptoms such as fever, general weakness, fatigue, muscle pain, headache, splenomegaly and hepatomegaly (Homer et al. 2000). However, severe pathology i. e. hemolytic anemia etc. is more likely to develop in immunocompromised individuals, patients who underwent splenectomy and also in elderly people (Homer et al. 2000). Treatment is based on an administration of clindamycin or atovaquone in combination with azithromycin (Krause et al. 2000, Wormser et al. 2006). Asymptomatic carriers could imperil immunocompromised individuals since no regulated test of blood donors for *Babesia* spp. were established before 2018. However, in 2018, The Food and Drug Administration (FDA) approved tests to screen blood donations for *B. microti* (FDA, Recommendations for Reducing the Risk of Transfusion-Transmitted Babesiosis, 2018).

1.2. *Babesia microti*

B. microti is classified into the basal lineage of piroplasms (*B. microti*-like group) (Fig. 1) and possesses several exceptions both in its lifecycle and in the selection of natural hosts compared to “true *Babesia*“ classified to *Babesia sensu stricto* lineage.

1.2.1. Natural hosts of *Babesia microti*

B. microti is characterized by two-host life cycle which involves a vertebrate (intermediate) host and a tick (definitive) host. The natural reservoir of *B. microti* is predominantly a white-footed mouse (*Peromyscus leucopus*). Approximately two-thirds of the population of *P. leucopus* harbour the parasite in endemic areas of the USA (Etkind et al. 1980). However, other small mammals such as raccoons, cottontail rabbits, voles, shrews, chipmunks, etc. are similarly considered as competent reservoirs (Hersh et al. 2012). The occurrence of *B. microti* was confirmed also in rodents in Europe (Sebek et al. 1977; Duh et al. 2001; Beck et al. 2011) and Asia (Rar et al. 2011).

Hard ticks from genus *Ixodes* are considered as definitive hosts of *B. microti*. *I. scapularis* is the principal tick host of the parasite in the USA (Yabsley and Shock 2013). In Europe

and also in Asia where *I. scapularis* is absent, analyses revealed the presence of *B. microti* in *I. ricinus* and *I. persulcatus* tick species, respectively (Duh et al. 2003; Zamoto-Niikura et al. 2016). Moreover, acquisition experiment with gerbils demonstrated that *I. ricinus* is a competent vector of *B. microti* (Gray et al. 2002).

1.2.1.1. *Ixodes ricinus*

Ixodes ricinus is a hard tick species which belongs to the genus *Ixodes*. The species can be found in Europe, Russia and also North Africa. Relatively wide geographical distribution of *I. ricinus* indicates the ability of this species to survive under various conditions. However, the tick mostly searches for humid habitats where it can encounter a variety of hosts suitable for all tick developmental stages (Alkishe et al. 2017). The tick has a three host lifecycle and has to take a blood meal in order to molt to the next stage. The lifecycle takes usually three years. The six-legged larva feeds on small/medium-sized vertebrates. The eight-legged nymph and adult females feed on large wild or domestic animals. Humans can be hosts of all tick instars (Sonenshine and Roe, 2014). *I. ricinus* is an important disease vector transmitting pathogens including viruses (tick-borne encephalitis flavivirus), bacteria (*Borrelia burgdorferi* sensu lato and *Anaplasma phagocytophilum*) and also protozoan parasites (*Babesia* spp.) (Sonenshine and Roe, 2014).

1.2.2. Life cycle of *Babesia microti*

The lifecycle of *B. microti* involves both asexual multiplication and sexual reproduction of the parasite. Merogony, first asexual multiplication, takes place in erythrocytes of the vertebrate host. Subsequent sexual reproduction, gamogony, occurs in the gut of the tick host. Later, the development continues in tick salivary glands where the parasite undergoes another round of asexual multiplication – sporogony (Jalovecka et al. 2018) (Fig. 2).

Multiplication in a vertebrate host: merogony

Once the tick infected with *B. microti* feeds on the vertebrate host, stages known as sporozoites are transmitted with tick saliva from salivary glands to the bloodstream of the vertebrate (Karakashian et al. 1983). After the internalization into red blood cells, sporozoites develop into trophozoites which later divide into merozoites. Subsequently, merozoites egress from the host cell and reinvade other healthy erythrocytes (Rudzinska et al. 1976; Jalovecka et al. 2018). The invasion of the host cells is a complex process involving probably a considerable number of proteins secreted from the apical complex of the parasite (Bargieri et al. 2014). *B. microti* orientates its apical (anterior) end with secretory organelles to close

contact with the host cell membrane (Rudzinska et al. 1976). Once *B. microti* is attached to the host erythrocyte by a junction mediated by proteins secreted from organelles of the apical end (Votycka et al. 2017; Rudzinska et al. 1976). After the establishment of the attachment, the membrane of the erythrocyte invaginates and starts forming a parasitophorous vacuole. However, in contrast to other Apicomplexan parasites, the parasitophorous vacuole of *Babesia* disappears shortly after the parasite internalization (Rudzinska et al. 1976). Merozoites of *B. microti* do not usually form a *Babesia*-typical tetrad formation called a Maltese cross which is, on the other hand, common for example for *B. divergens* or *B. bovis*. The shape of the merozoites of *B. microti* is not uniform since they form pseudopods or invaginations (Rudzinska et al. 1976).

Except for all aforementioned asexual stages, there are also stages referred as gametocytes in the host blood which are predetermined to evolve into gametes later in the lumen of the tick gut (Rudzinska et al. 1979, Becker et al. 2010). Once they differentiate, gametocytes do not replicate in the host erythrocytes and wait for being ingested with the blood meal by the tick host. The driven mechanisms of *Babesia* sexual commitment is not so far known (Jalovecka et al. 2016).

Multiplication in a tick host: gamogony and sporogony

When the tick starts feeding there is a mixture of asexual stages (merozoites) and sexual stages (gametocytes) in the tick gut lumen. While merozoites rapidly degrade, gametocytes released upon the erythrocyte lysis finish their development freely in the lumen. Occasionally, they mature still within ingested erythrocytes (Rudzinska et al. 1979; Rudzinska et al. 1984). Then, gametocytes metamorphose and produce gametes which are according to morphological traits called spiky-rayed stages or Strahlenkörper (Mehlhorn and Schein 1993). Gametes of *B. microti* are divided into two populations which acquire minor differences in the cytoplasm density. Nonetheless, using light microscopy, they cannot be distinguished. Therefore, the typical differentiation and appellation as a micro and macrogamete are not applicable for *B. microti* (Rudzinska et al. 1979).

Fertilization and zygote formation occurs when two gametes of a different type connect via filamentous protrusions and subsequently one gamete penetrates the other (Rudzinska et al. 1983). Firstly, the newly emerged motile zygote termed as ookinete passes across the peritrophic matrix which is a temporarily formed membrane separating the content of the tick gut lumen and the gut wall. Secondly, zygote actively invades gut epithelial cells using organelle known as an arrowhead. The parasite is encircled by an invaginating membrane

of the gut epithelial cells. Subsequently, the membrane disintegrates and the zygote is surrounded solely by the cytoplasm of the epithelial cell. Arrowhead changes its morphology which suggests the release of molecules required during the invasion (Rudzinska et al. 1982).

Finally, in the cytoplasm of epithelial cells, zygote goes through meiotic division which leads to a formation of haploid kinetes. Kinetes of *B. microti* are considered as invasive stages since they invade intra-tick organs i. e. nephrocytes, fat body or salivary glands upon the release from the gut epithelial cells (Karakashian et al. 1986). In tick tissues, the kinetes asexually multiply and form secondary kinetes. Unlike species of *Babesia* sensu stricto group, *B. microti* does not invade ovaries. Therefore, *B. microti* is transmitted solely transstadially (Jalovecka et al. 2018).

Sporogony, the asexual reproduction, is a next phase of *B. microti* lifecycle within the tick host. (Karakashian et al. 1983). Initially, secondary kinetes colonize acini of salivary glands where they transform into a single-membrane syncytium known as a sporont. Next, the sporont develops into multinucleated meshwork – sporoblast. This occurs before the tick moulting and sporoblast stays dormant until the next instar of the tick starts feeding on the vertebrate host. When the tick attaches to the host, maturation of the sporoblast is initiated and the apical complex is formed before fully mature sporozoites are released (Karakashian et al. 1983). Sporozoites arise via multiple fissions and can be released with tick saliva into the host bloodstream where they invade the naïve erythrocytes (Rudzinska et al. 1976; Karakashian et al. 1983).

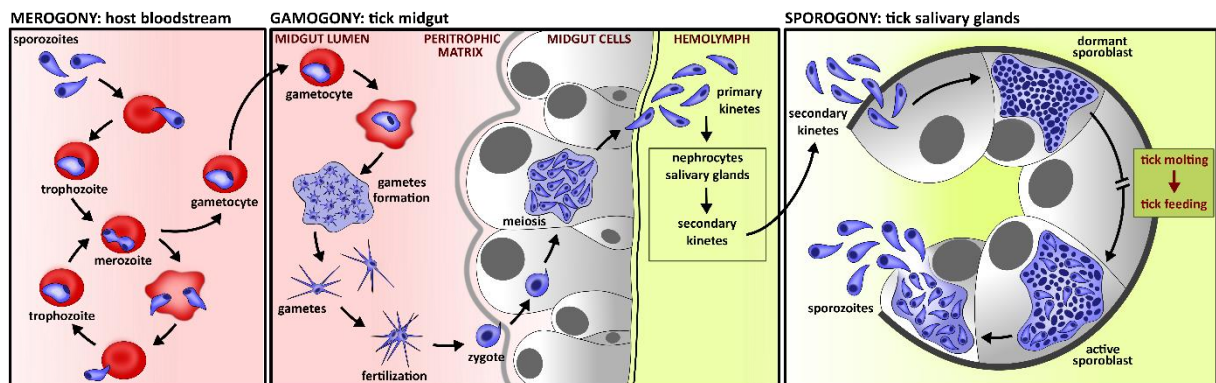


Figure 2: Lifecycle of *B. microti*. During the tick feeding, sporozoites are transmitted with saliva from tick salivary glands to a bloodstream of a vertebrate host. Sporozoites invade erythrocytes where subsequent asexual multiplication - merogony - takes place. Sexual commitment when first sexual stages – gametocytes – emerges occurs in the bloodstream. Gametocytes are ingested together with the blood meal mature and produce gametes in the tick gut lumen (gamogony). Newly emerged gametes fuse in a zygote which passes across the peritrophic matrix into tick gut epithelial cells. Meiotic division gives rise primary kinetes which multiply in different tick tissues. Secondary kinetes invade salivary glands where sporogony occurs (Jalovecka et al. 2018).

1.2.3. Apical complex

Members of the phylum Apicomplexa are characteristic for a unique organization of the organelles in the anterior pole of their cell (Votypka et al. 2017). These organelles together constitute a formation termed apical complex. Generally, the complex comprises of secretory claviform rhoptries, filamentous micronemes and dense granules. Although the latter are located more distantly from the apical end of the cell (Votypka et al. 2017). The organelles supply molecules necessary for the cell motility, for the adhesion to host cells and their invasion, as well as for the development of a parasitophorous vacuole (Morrisette and Sibley 2002). A conoid and polar ring(s) are other, however, non-secretory organelles of the complex (Votypka et al. 2017).

The order Piroplasmida is characterized by a noticeably reduced apical complex. The conoid is completely missing (Votypka et al. 2017). Particularly, *B. microti* possesses the most reduced complex within piroplasmids (Jalovecka et al. 2019). It comprises of a single large rhoptry, a few micronemes and a spherical body – an organelle analogous to the dense granules of other apicomplexan parasites (Jalovecka et al. 2018). Polar rings and subpellicular microtubules are absent (Rudzinska and Trager 1977). Organelles of the complex can be found in all invasive stages of *B. microti* i. e. sporozoites, merozoites (Fig. 3) and kinetes. However, kinetes lack large rhoptry (Rudzinska and Trager 1977; Karakashian et al. 1983; Karakashian et al. 1986).

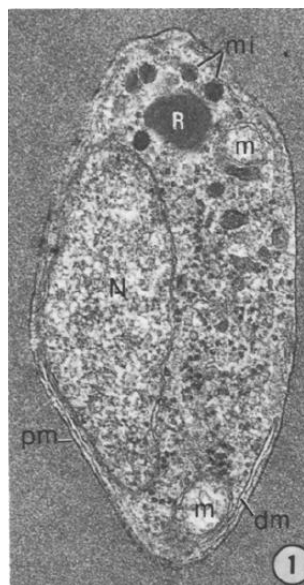


Figure 3: *B. microti* merozoite inside erythrocyte. Note a plasma membrane (pm), segments of double membranes under the plasma membrane (dm), a large rhoptry (R) and several micronemes (mi) in the apical end of the cell, two mitochondria (m) and a large nucleus (N). Magnification: 45 000× (Rudzinska and Trager 1977).

1.3. Apical membrane antigen 1 (AMA-1)

AMA-1 is a micronemal protein extensively studied within the phylum Apicomplexa. The phylogenetic comparison shows that *ama-1* gene sequence clusters depending on the genus (Crawford et al. 2010; Jiang et al. 2012). Despite the differences in host and tissue specificity, the function of the protein seems to be universal throughout the phylum Apicomplexa (Tyler et al. 2011). AMA-1 is suggested to be one of the key elements involved in the process of host cell invasion of apicomplexan parasites (Triglia et al. 2000; Mital et al. 2005; Montero et al. 2009). Therefore, it has also become one of the potential candidates included in the anti-malarial vaccine (Remarque et al. 2008).

1.3.1. Structure of AMA-1

The protein consists of an intracellular C-terminal sequence, a single transmembrane region and an N-terminal ectodomain. The ectodomain typically contains 16 conserved cysteines which divide it by disulphide bonding into three domains – DI, DII and DIII. This structural organization was described in *Plasmodium falciparum* (Hodder et al. 1996; Pizarro et al. 2005), *Toxoplasma gondii* (Hehl et al. 2000) and also *B. divergens* (Montero et al. 2009). Although AMA-1 homolog was identified in *B. microti*, protein differs from that of *B. divergens* by a lack of two cysteines in DIII (Moitra et al. 2015).

1.3.2. Role of AMA-1 in host cell invasion

AMA-1 has been studied as one of the important ligands in moving junction which is a protein complex facilitating the host cell invasion by apicomplexan parasites. Proposed protein interactions in the junction involve also the complex of rhoptry neck proteins (RONs), a receptor for AMA-1 (Vulliez-Le Normand et al. 2012) (Fig. 4). As described on two model apicomplexan species, *T. gondii* and *Plasmodium falciparum*, AMA-1 is secreted from micronemes and interact with RONs secreted from rhoptries into the host cell (Besteiro et al. 2009; Lamarque et al. 2011; Vulliez-Le Normand et al. 2012). The interaction of AMA-1 and RON2 appeared to be crucial for host cell invasion since antibodies or peptides preventing this interaction significantly reduced the invasion by *Plasmodium* merozoites (Collins et al. 2009; Richard et al. 2010), and *Toxoplasma* tachyzoites (Tyler and Boothroyd 2011). Moreover, anti-AMA-1 antisera inhibited invasion of red blood cells by *B. bovis* merozoites *in vitro* by approximately 65% (Gaffar et al. 2004). Corresponding results of the inhibition using antibodies *in vitro* were reported both for *B. divergens* (Montero et al. 2009) and *B. microti* merozoites (Moitra et al. 2015). Wang et al (2017) reported depletion of invasion

in hamsters infected with *B. microti* when they were formerly immunized by a combination of AMA-1 and RON2 recombinant proteins (Wang et al. 2017).

However, the contradiction results have been demonstrated with *ama-1* knock out assay on tachyzoites of *T. gondii* and merozoites of *Plasmodium berghei* which did not display any impairments in the host cell invasion. Nevertheless, the efficiency of invasion was decreased due to altered zoite adhesion properties. This result suggests that AMA-1 is probably not essential in the formation of moving junction yet it can be a part of it. Rather AMA-1 can be involved in the cell positioning, host cell-binding step or possibly in rhoptry secretion (Bargieri et al. 2013).

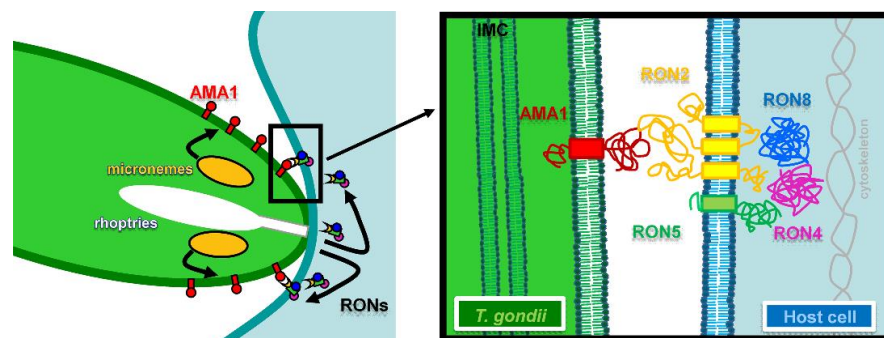


Figure 4: Scheme of the organization of moving junction in *T. gondii*. AMA-1 is anchored in the parasite membrane while RON proteins are transported and exposed on the surface of the host cell (Besteiro et al. 2009).

1.3.3. AMA-1 in the lifecycle of apicomplexans

AMA-1 is associated with the presence of apical secretory organelles in apicomplexan parasites. Therefore, the protein is primarily discussed as a surface marker specific for invasive stages which use the apical complex during asexual multiplication in a vertebrate host (Donahue et al. 2000; Bannister et al. 2003; Moitra et al. 2015).

However, the organelles of the complex can be found also in other developmental stages for which the invasive progression is typical. Predictably, AMA-1 was identified in invasive sporozoites of several apicomplexan species. For example, AMA-1 of *P. falciparum* is expressed on the surface of sporozoites during the invasion of hepatocytes. Nevertheless, the protein is lost during subsequent development. Moreover, antibodies targeting AMA-1 of sporozoites inhibit the invasion of hepatocytes *in vitro* (Silvie et al. 2004). On the other hand, AMA-1 of *Plasmodium berghei*, which is also expressed in sporozoites, was confirmed to be dispensable for these stages since both knockdown and knockout of the gene did not prevent the parasite from the invasion of hepatocytes (Giovannini et al. 2011; Bargieri et al. 2013). Sporozoites of *T. gondii* use for the invasion of host cells a paralogue of AMA-1

protein instead (Poukchanski et al. 2013). AMA-1 was detected also in sporozoites of *Eimeria tenella* (Jiang et al. 2012). The protein has not been studied in sporozoites of *B. microti* so far. Since the apical organelles such as micronemes and rhoptries are present in these stages, possible expression of the protein cannot be dismissed (Karakashian et al. 1983).

Up to now, no study elucidated whether the AMA-1 expression is specific also for intra-tick invasive stages of *B. microti*. Based on the fact that kinetes can invade the tissues of the tick host and that they possess numerous micronemes within the anterior part of their cells, the occurrence of AMA-1 could be also probable (Karakashian et al. 1986).

Unexpectedly, AMA-1 was determined also in some of the gametocytes of *E. tenella*. The expression increased at the beginning of sexual reproduction. Nevertheless, it decreased when the parasite developed into an unsporulated oocyst. The result suggests that AMA-1 is probably expressed in a microgamete which enters a macrogamete to form a zygote. Hypothetically, this would indicate that AMA-1 is involved not only in the host cell invasion but also in the “self-invasion” (Jiang et al. 2012).

Overall, AMA-1 expression is probably connected with the invasive behaviour of different stages throughout the lifecycles of apicomplexan parasites. Nonetheless, the presence and the role of AMA-1 in some of them is yet to be investigated.

1.4. CCp2

CCp proteins are classified as a family of secreted proteins which share conserved adhesive domains including at least one *Limulus* coagulation factor C (LCCL) domain (Trexler et al. 2000; Dessens et al. 2004). The proteins were studied primarily in *P. falciparum* (Lasonder et al. 2002; Pradel et al. 2004). Nonetheless, gene orthologues have been identified in various apicomplexan parasites (Dessens et al. 2004; Tosini et al. 2006; Bastos et al. 2013). CCp proteins are probably involved in parasite-parasite adhesion interaction during sexual development (Kuehn et al. 2010; Becker et al. 2013).

In *P. falciparum* the protein expression was proven to be gametocyte and gamete-specific, and no expression was detected in asexual stages. *In vitro* experiments revealed that CCp proteins are surface associated and can be localized within the gametocyte parasitophorous vacuole (Kuehn et al. 2010). During gametogenesis in the mosquito midgut, CCp proteins are present on the surface of gametes. Conversely, the gene expression was decreasing after egression. Zygote displayed low expression and later, no signal was detected on the surface of ookinetes (Pradel et al. 2004). Knock-out of *ccp2* and *ccp3* genes did not have any adverse

effect neither on parasite gametocytogenesis and oocyst formation nor the development of sporozoites within the oocyst. However, no sporozoites could be localized in the hemolymph and salivary glands of the mosquito. This implies that the transition of sporozoites from the oocyst was in some way aborted. (Pradel et al. 2004). Interestingly, CCp proteins were detected in proteome of sporozoites of *Cryptosporidium parvum* and their secretion was suggested from micronemes (Tosini et al. 2004; Snelling et al. 2007). The authors also hypothesize on the adhesion function of CCp proteins during sporozoite invasion of the host cells (Tosini et al. 2004).

Sexual stages of *Babesia* spp. are difficult to recognize based on morphology analysis compared to the stages of *P. falciparum*. Therefore, CCp proteins have become promising sexual stage-specific molecular markers of *Babesia* spp. Based on the sequence of *ccp* genes of *P. falciparum*, three orthologues (*ccp 1-3*) have been identified in *B. divergens*, *B. bigemina* and *B. bovis*. Transcription of the genes was described in gametocytes of all aforementioned *Babesia* species (Becker et al. 2010; Bastos et al. 2013). The protein expression was demonstrated only in the sexual stages of *B. bigemina* induced *in vitro*. This, however, does not have to imply for non-induced blood stages *in vivo*. No protein expression was detected in *B. bovis* blood or tick stages (Bastos et al. 2013). To the contrary, the presence of CCp2 protein was validated in the sexual stages of *B. divergens* in the gut of engorged females of *I. ricinus* using anti-CCp2 antibodies. Yet, it is difficult to conclude whether the CCp2 protein secretion is only gametocyte or also gamete and zygote specific (Becker et al. 2013). To date, CCps have not been studied in the sexual stages of *B. microti* but probably the similar pattern of the protein expression would be anticipated.

2. Objectives

1. Quantification of *B. microti* in tick tissues in the course of blood-feeding.
2. Quantification of the gene expression of selected surface markers of *B. microti* in tick tissues.
3. Synthesis of fragments of selected surface markers of *B. microti* and preparation of polyclonal antibodies.
4. Immunodetection of *B. microti* developmental stages in both the vertebrate and the tick host.
5. Assessment of immunogenicity of one of the selected markers.

3. Material and Methods

3.1. Parasite and laboratory animals

B. microti (Franca) Reichenow (PRA-99TM), strain Peabody mjr. was purchased from ATCC[®]: The Global Bioresource Center, and propagated *in vivo* in BALB/c mice. *I. ricinus* nymphs were supplied by the tick breeding facility of the Institute of Parasitology, BC CAS, and kept under constant conditions (25°C, 95% humidity). *Mus musculus* - BALB/c female mice (6 week-old) and the rabbit breed Hyplus (3 month-old) were obtained from VELAZ inc., Czech Republic. Throughout all experiments mice and the rabbit were kept in the animal facility of the Institute of Parasitology, BC CAS. All experimental animals were treated in accordance with the Animal Protection Law of the Czech Republic No. 359/2012 Sb. and with the decree 419/2012 Sb. of Ministry of Agriculture on the protection of experimental animals (including relevant EU regulations).

3.2. Propagation of *B. microti* in BALB/c mice

B. microti strain was propagated in BALB/c mice by passaging. Firstly, the mouse was intraperitoneally (i.p.) injected with defrosted *B. microti* infected murine blood (200 µl). When the parasitemia reached 5-10%, mouse was injected (i.p.) with 130 µl of anesthetic solution, mixture of 5% Narkamon (Spofa, Czech Republic), 2% Rometar (Spofa, Czech Republic) and 1 × PBS (Phosphate Buffered Saline, pH 7.3) in ratio 4:1:5, respectively, and the blood was obtained by cardiac puncture procedure. The blood was mixed with sodium citrate-phosphate-dextrose solution (Sigma-Aldrich, USA) in 1:7 ratio, and 150 µl of the mixture was injected i.p. to another mouse. After the mouse reached the peak of infection (usually ~45% parasitemia on the 6th day post-infection) the blood was taken using the same procedure. Then, blood was injected into experimental mice again (Fig. 5). In case all blood was not passaged, the rest was carefully mixed with 30% glycerol in Alsevere solution (Sigma-Aldrich, USA) in ratio 2:1. The mixture was incubated on ice for 15 minutes and subsequently frozen in liquid nitrogen. Later, the strain could be defrosted and used for passage.

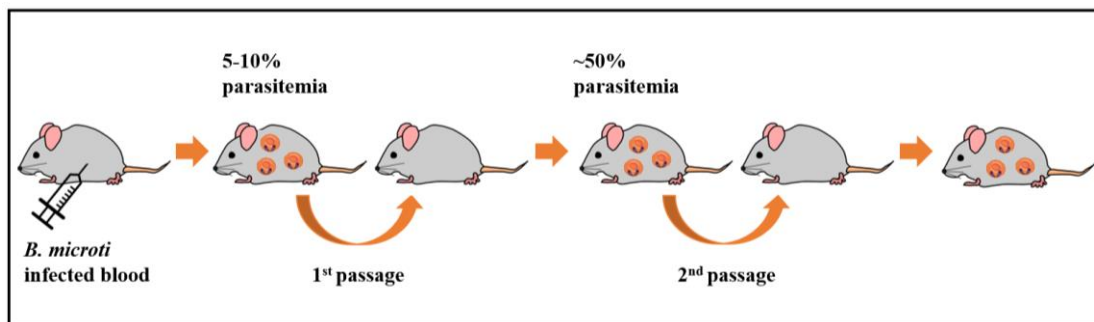


Figure 5: Propagation of *B. microti* in BALB/c mice by passaging.

3.3. Determination of parasitemia of *B. microti* in murine blood

The level of parasitemia in blood was determined from blood smears. Blood smears were prepared from a 5 µl-drop of blood taken from the partly cut tail of the mouse. Slides with the blood smears were air-dried and stained with Diff-Quik staining set (Siemens, Germany), rinsed with 70% ethanol and distilled water. Next, slides were observed with an Olympus BX53 microscope under 100× objective (1000× magnification). Photos were taken with Olympus DP72 camera and CellSens imaging software. Parasitemia was counted as a number of *B. microti* infected erythrocytes per 1000 erythrocytes.

3.4. Tick maintenance and feeding set up

Up to 20 *I. ricinus* nymphs were placed into a plastic cup which was beforehand mounted on the back of BALB/c mouse (either *B. microti* negative control mouse or *B. microti* infected mouse which was i.p. injected with 150 µl of infected blood ~50% parasitemia). Nymphs started feeding on the *B. microti* infected mice in two different time points depending on the level of parasitemia in the blood (Fig. 6). The first group started feeding on the 1st day post-infection (1DPI) in the acute phase of infection. The second group started feeding on the 5th day post-infection (5DPI) at the beginning of the decline phase of infection. To get a homogenous group of engorged ticks, the nymphs which did not start feeding after four hours from the placement into the cup were removed. Subsequently, nymphs were removed from mice in three timepoints of feeding i.e. after 24 hours = one day post attachment (1DPA), after 48 hours = two days post attachment (2DPA) and 72 hours = three days post attachment in fully engorged stage (3DPA). Additionally, part of the nymphs removed in the fully engorged stage was left for another 6 days. Therefore, last time point was set on the sixth day post-detachment (6DPD) (Fig. 6).

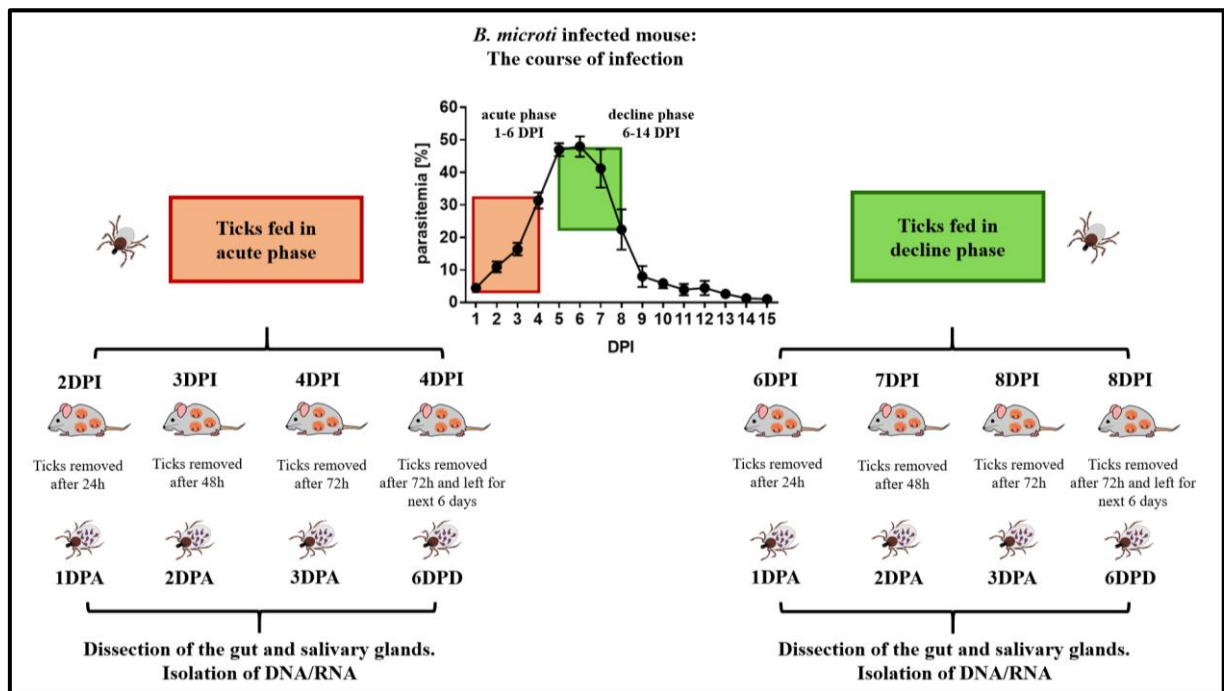


Figure 6: Set up of the tick feeding on mice with different levels of parasitemia. Nymphs started feeding on mice either in the acute phase of infection (1DPI) or at the top of infection (5DPI). Nymphs were removed after 24, 48 and 72 hours of feeding (1, 2, 3 DPA, respectively). Part of the group which was removed after 72 hours was left for another 6 days (6DPD). DPI = days post-infection. DPA = days post attachment. DPD = days post-detachment.

3.5. DNA extraction

Genomic DNA for absolute quantification was isolated from nymphs which were treated as stated in chapter 3. 4. DNA was isolated from a single salivary gland and gut of *B. microti* positive nymphs (10 nymphs/time point) using NucleoSpin® Tissue kit and the manufacturer's protocol (Macherey-Nagel, Germany). DNA isolated from salivary glands was also tested for DNA contamination from murine blood (using *M. musculus* specific primers; see Table 3). Positive samples which were contaminated during dissection were excluded from the experiment.

Samples, which were used as controls for subsequent experiments namely DNA from *B. microti* negative nymphs and *B. microti* positive and negative blood were isolated according to the manufacturer's protocol using either NucleoSpin® Tissue kit or NucleoSpin® Blood kit (Macherey-Nagel, Germany). DNA isolation was verified using either *Ixodes* spp. or *M. musculus* control primers.

3.6. RNA extraction and cDNA synthesis

Total RNA for relative quantification was isolated from salivary glands and the gut of the *I. ricinus* nymphs which were removed from either *B. microti* positive mice or control *B. microti* negative mice in the aforementioned time points (see 3.4.). For each time point (1DPA, 2DPA, 3DPA and 6 DPD), dissected guts of the 10 nymphs were pooled. Salivary glands were treated equally. The pooling of the tissues was done identically for *B. microti* positive nymphs and for *B. microti* negative nymphs.

Except for the elution volume which was adjusted to 40 µl, the isolation of RNA was proceeded according the manufacturer's protocol using NucleoSpinRNA II kit (Macherey-Nagel, Germany). RNA for the relative quantification was isolated also from *B. microti* positive blood. The blood was sampled in sodium citrate-phosphate-dextrose solution (1:7 ratio). RNA was isolated using the same protocol and kit as RNA from the tissues. In case of persisting DNA contamination, RNA was treated with TURBO DNA-free™ Kit (Invitrogen, USA) and DNA contamination was excluded by PCR. RNA was stored at -80°C prior to cDNA synthesis. Single-stranded cDNA was reverse-transcribed from 1 µg of total RNA according to the manufacturer's protocol using Transcriptor High-Fidelity cDNA Synthesis Kit (Roche, Switzerland). For subsequent applications, cDNA was diluted 5× in nuclease-free water (Top-Bio, Czech Republic).

3.7. PCR and gel electrophoresis

Polymerase chain reactions (PCR) were executed in Mastercycler gradient (Eppendorf, Germany). Reaction was usually of volume of 25 μ l (Table 1). The primers used are listed in Table 3. The program generally used is depicted in Table 2. PCR products were separated on Ethidium Bromide (Sigma-Aldrich, USA) stained 1% agarose gel consisting of Agarose DNA Pure Grade (VWR, Belgium) and 1 \times TAE buffer (40 mM Tris-acetate, 1 mM EDTA, pH 8.0). 2% agarose gel was used in case the products were of the size about 100 bp. PCR samples were loaded in the mixture with 6 \times DNA Gel Loading Dye (Thermo Fisher Scientific, USA) and visualized using Gel logic 112 transluminator (Sigma-Aldrich, USA). Size of the PCR products was determined using GeneRuler™ 100bp DNA Ladder (Thermo Fisher Scientific, USA).

Table 1: Standard PCR reaction set-up.

Reagent	Volume
FastStart™ PCR Master (Roche, Switzerland)	12.5 μ l
Forward primer (10 μ M)	1 μ l
Reverse primer (10 μ M)	1 μ l
DNA/cDNA	4 μ l
Nuclease-free water (Top-Bio)	6.5 μ l

Table 2: Standard PCR amplification program.

	Temperature	Time	
Initial denaturation	94°C	10 min	} 40 \times
Denaturation	94°C	30 sec	
Annealing temperature	60°C	30 sec	
Elongation	72°C	60 sec	
Final elongation	72°C	7 min	

Table 3: List of primers used in experiments.

Organism and gene specification - reference number (NCBI)	Primer sequence (5' - 3') and amplicon length (bp)		Usage *internal reference number	Primers adapted from/designed by
<i>B. microti ama-1</i> JX488467 #	F: TTAAGCCTCAATGGCTCGAT R: GGTAGCCTGCGCAAAAATA	1644	Sequencing * IR1053 * IR1054	
<i>B. microti ccp2</i> XM_012793659 #	F: TAGGGGAACCTGATGCTTTG R: TTCCGGCCATTTCTTTAGTG	1632	Sequencing * IR1061 * IR1062	
<i>I. ricinus ferritin2</i> AF068224	F: TCAGCTCATGGACTTCATCG R: ATTCGCTGCAGCTTGCAAT	72	Standard for <i>B. microti</i> quantification *IR92 *IR93	Hajdušek, O. (unpublished)
<i>B. microti ama-1</i> JX488467	F: ATTCAACTGCGCTCCTATG R: TGGATTAGTTGCAACGGAGA	132	Absolute/ relative quantification *IR443 *IR444	Jalovecka, M., 2017
<i>B. microti ccp2</i> XM_012793659	F: TATGGGATTCAGCGCCTTTA R: TCACTTCTACGACGCTTTCG	135	Relative quantification *PK485 *PK486	
<i>B. microti actin</i> XM_012791652	F: GGCCTACTCACAGCCCTTTA R: ACAGGGTTGTAGAGTGTGGTT	135	Relative quantification *PK571 *PK572	
<i>Babesia</i> spp. 18S	F: AACCTGGTTGATCCTGCCAGTAGTCAT R: GAATGATCCTTCCGCAGGTTACCTAC	1728	Nested PCR 1 st reaction *IR270 *IR275	(Malandrin et al. 2010)
<i>Babesia</i> spp. 18S	F: GYYTTGTAATTGGAATGATGG R: CCAAAGACTTTGATTCTCTC	560	Nested PCR 2 nd reaction *IR272 *IR273	
<i>B. microti ama-1</i> JX488467	F: CACCACTGCCAAAACACTGAAAGCA R: CTATGCAATGTTCCCATCTTGA	650	Cloning *PK503 *PK504	
<i>B. microti ccp2</i> XM_012793659	F: CACCCCGTGGCATTATAT R: CTATCCGATGCCAGTATCCTTC	650	Cloning *PK505 *PK506	
<i>Ixodes</i> spp. <i>nexin 24</i> (XM_002435546)	F: GAGGCATGAGGGTGTGTTTT R: GACCTGCACGAAAATGATTG	600	DNA extraction control	Šíma, R. (unpublished)
<i>M. musculus</i> <i>chromosome 2</i>	F: GCTTCTGGAAGAACCACAGG R: AAGCACTTCGAACCACTGCT	600	DNA extraction control	

Annealing temperature of all primers was 60°C; bp = base pairs.

3.8. Quantitative PCR

3.8.1. Absolute and relative quantification

Number of *B. microti* present in tissues of *I. ricinus* nymphs during and post feeding was assessed using DNA which was isolated as stated in the chapter 3. 5. Expression of *ama-1* and *ccp2* genes was measured using cDNA which was prepared as specified in the chapter 3.6. Samples were analyzed in technical triplicates in LightCycler® 480 Instrument II (Roche, Switzerland). Reaction was prepared as indicated in Table 1 using FastStart Universal SYBR Green Master instead (Roche, Switzerland). Amplification program used is depicted in Table 4. Two independent experiments (biological duplicates) were carried out to analyze respective gene expression in given timepoints.

Absolute quantification was based on the standard curves for *ama-1* (JX488467) and *ferritin2* (AF068224) genes which were previously implemented (Jalovecka 2017). Number of parasites was normalized to 10^3 tick genomes (*ferritin2* gene). Relative quantification of *ama-1* and *ccp2* mRNA was normalized to babesial *actin* gene (XM_012791652) using the $\Delta\Delta C_t$ method (Pfaffl 2001). Assay results were analyzed in LightCycler480 Software, version 1.5 (Roche, Switzerland). Data were analyzed by GraphPad Prism 6 for Windows, version 6.04.

Table 4: Amplification program used for absolute and relative quantification.

	Temperature	Time	
Initial denaturation	95°C	5 min	} 55×
Denaturation	95°C	20 sec	
Annealing	60°C	30 sec	
Elongation	72°C	30 sec	

3.9. Cloning of *ama-1* and *ccp2* genes

Coding sequence of *ama-1* and *ccp2* gene (JX488467, XM_012793659, respectively) was validated by sequencing (SEQme inc., Czech Republic) using sequencing primers (IR1053, IR1054 and IR1061, IR1062). Primers were designed on the basis of *ama-1* and *ccp2* gene sequence available in GenBank database. Prior cloning, external region of AMA-1 transmembrane protein and corresponding part of the gene sequence was determined using TMHMM Server, v. 2.0 (Fig. 7).

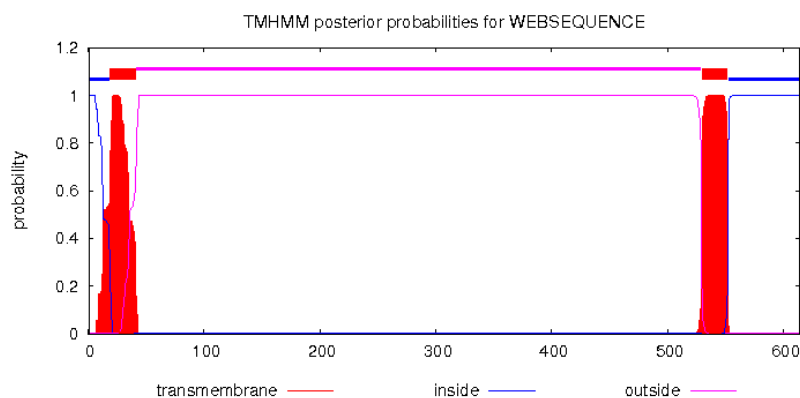


Figure 7: Prediction of AMA-1 external region using TMHMM Server. The predictor suggested two transmembrane helices in AMA-1 protein (transmembrane). External region comprises of 488 amino acids (outside).

Sequences selected for cloning were amplified using High Fidelity PCR Enzyme Mix, dNTPs (Thermo Fisher Scientific, USA), nuclease free water and specific primers for cloning (PK503, PK504; PK505, PK506). cDNA from *B. microti* positive blood served as a template. PCR reaction and amplification program was set up according manufacturer's protocol supplied with the enzyme mix. TOPO[®] cloning reaction and transformation of competent TOP10 *Escherichia coli* cells with pET100/D-TOPO vector (Fig. 8) were conducted using manufacturer's protocol and Champion[™] pET Directional TOPO[®] Expression Kit (Invitrogen, USA).

TOP10 *E. coli* cells were cultured on Luria-Bertani (LB) broth plates supplemented with ampicillin (LB-amp) (37°C; 12 hours). Plates were prepared using 10 g of broth (Amresco, USA), 6 g of agar (Amresco, USA), 400 ml of distilled water and ampicillin with final $c = 50 \mu\text{g/ml}$. Grown colonies were tested for the presence of the inserted sequence in the vector using PCR. Positive *E. coli* colonies were inoculated into 4 ml of LB-amp medium and incubated (37°C; 200 rpm; 15 hours). The vector containing the target sequence was isolated according to the manufacturer's protocol using High Pure Plasmid Isolation Kit (Roche, Switzerland) and sequenced (SEQme inc., Czech Republic).

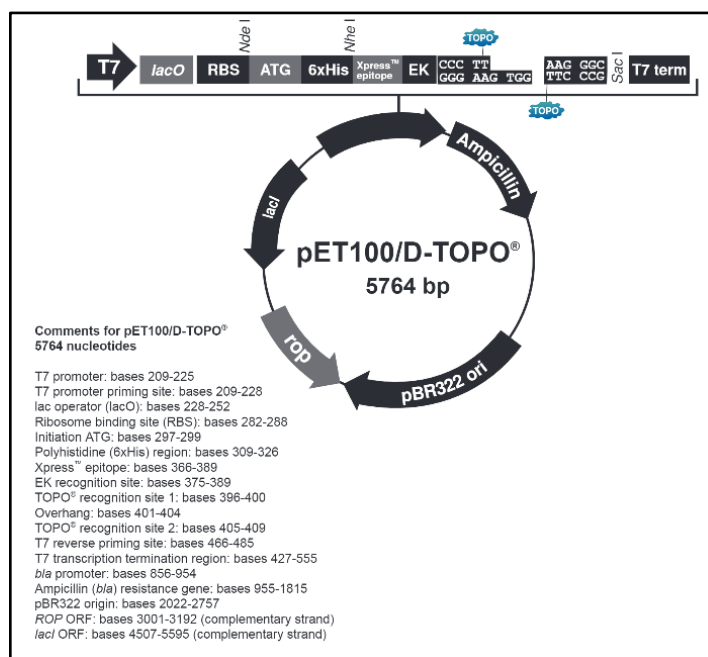


Figure 8: Expression vector pET100/D-TOPO[®]. Adapted from Champion™ pET Directional TOPO[®] Expression Kits protocol (Invitrogen, USA).

3.10. Expression and purification of AMA-1 and CCp2 recombinant proteins

Using the manufacturer's protocol, One Shot™ BL21 Star™ (DE3) chemically competent *E. coli* cells (Invitrogen) were transformed with pET100/D-TOPO vector containing verified sequence of interest. Bacterial suspension was spread over LB-amp plates. Next, one colony of cells was inoculate cultivated in 400 ml of LB-amp supplemented with 1M glucose (37°C; 200 rpm; 8 hours). Subsequently, cells were centrifuged (3000g; 10 min) and washed in LB-amp medium to get rid of the glucose. Procedure was repeated twice. Protein expression was induced by adding IPTG (Isopropyl-β-D-thiogalaktopyranozide, c = 0.5 mM; Thermo Fisher Scientific, USA). After 12-hour cultivation (37°C; 200 rpm), cells were centrifuged.

To isolate proteins from the cells, bacterial pellet was resuspended in solubilisation buffer (6M guanidine – hydrochloride, 20 mM Tris-HCl, 0.5 M NaCl, 10 mM imidazole, 1 mM mercaptoethanol; pH 8.0) by shaking overnight in 4°C. Next, proteins were purified using chelating chromatography which is based on affinity interaction of Ni²⁺ ions on Hi-Trap™ IMAC FF column (GE Healthcare, USA) and His-Tag of the recombinant protein. Purification was conducted in the buffer A (8 M urea, 50 mM Tris, 0.5 M NaCl; pH 7.8). Recombinant proteins were eluted from the column with increasing concentration of the buffer B (8 M urea, 50 mM Tris, 0.5 M NaCl, 0.5 M imidazole; pH 7.8). The protein yield was evaluated by spectrophotometry and fractions of the highest concentration were analyzed with SDS-PAGE.

3.11. Protein refolding

To remove urea and to obtain proper tertiary structure of the protein, purified fractions were mixed and dialyzed in ViskingR dialysis tubing 16 mm membrane (Serva, Germany) against a series of 4 refolding buffers with decreasing concentration of urea (50 mM Tris-HCl, 0.5 M NaCl, 20% glycerol and urea - 4M, 2M, 1M and no urea). Fractions were dialyzed in 4°C for 12 hours in each refolding buffer.

3.12. Rabbit immunization and preparation of polyclonal antibodies

The rabbit was immunized with 100 µg of refolded AMA-1 recombinant protein diluted in 500 µl of either complete (first immunization) or incomplete (second and third immunization) Freund's adjuvant (1:1 ratio) (Sigma-Aldrich, USA). Volume of the protein was adjusted with 1 × PBS. Immunization was repeated 3 times in two-week intervals. 14 days post last challenge, rabbit blood was collected. Blood was incubated for 2 hours at room temperature and overnight in 4 °C. Subsequently, serum was separated by centrifugation (4°C; 870g; 15 min).

3.13. Reducing SDS PAGE and Western blot

Recombinant proteins were analyzed by SDS-PAGE using either NuPAGE 4 – 12% Bis-Tris Protein Gel (Thermo Fisher Scientific, USA) or Criterion™ TGX Stain-Free™ Precast Gel (Bio-Rad, USA). Coomassie Brilliant Blue staining was used for visualization. For Western blot, gel loads were electro-blotted to a polyvinylidene difluoride membrane using the Trans-Blot Turbo system (Bio-Rad, USA). The membrane was blocked in 1% non-fat skimmed milk in 1 × PBS with 0.05% Tween 20 (PBS-T; Sigma-Aldrich, USA) overnight (4°C). For immunostaining the membrane was exposed to primary antibody (1 hour). The primary antibody was either Anti-His-Tag (Sigma-Aldrich, USA) diluted by 1:1000 or Anti-AMA-1 serum diluted by 1:5000, 1:2000 and 1:1000 in 1% non-fat skimmed milk in 1 × PBS-T. The membrane was washed in PBS-T (3 × 5 min), and subsequently exposed (1 hour) to either Anti-Mouse IgG-peroxidase secondary antibody (in case of anti-His-Tag primary antibody; Sigma-Aldrich, USA) or Anti-rabbit IgG-peroxidase secondary antibody (in case of rabbit serum; Sigma-Aldrich, USA) diluted by 1 : 2000 in 1% non-fat skimmed milk in 1 × PBS-T. After the final wash in PBS-T (4 × 5 min), the membrane was visualized in ChemiDoc™ Imaging System (Bio-Rad, USA) using the ClarityWestern ECL substrate (Bio-Rad, USA).

3.14. Preparation of the blood samples and tick gut samples for immunolocalization of *B. microti*

Smears of *B. microti* positive murine blood (6DPI, the peak of infection) were air-dried on the Superfrost Plus™ Adhesion Microscope Slides (Thermo Fisher Scientific, USA) and fixed with 4% paraformaldehyde (30 min). Samples were washed in 1 × PBS (3 × 5 min) and incubated in 1% bovine serum albumin + 10% goat serum in 0.3% PBS-T (45 min). Primary antibody (anti-AMA-1 serum or serum collected from non-immunized rabbit diluted by 1:100 in 0.3% PBS-T) was applied (1 hour). The wash in 0.3% PBS-T (3 × 7 min) and incubation in secondary antibody (Goat Anti-Rabbit IgG H&L Alexa Fluor®647; Invitrogen - Thermo Fisher Scientific, USA) (1 hour) followed. Slides were washed in 0.3% PBS-T (2 × 5 min), after that incubated in 300 nM DAPI in 1 × PBS (5 min), washed again in 1 × PBS (2 × 5 min). Eventually slides were mounted in Fluoromount medium (Sigma-Aldrich, USA). Smears of uninfected murine blood and smears of *B. microti* positive murine blood with only secondary antibody applied served as controls. Guts were dissected from fully fed nymphs feeding on the mouse in the decline phase of infection. Gut epithelium and lumen content were spread on the Superfrost Plus™ Adhesion Microscope Slides. Samples were treated the same way as blood smears. Tick gut of fully fed uninfected nymphs served as a control.

3.15. Repeated infections of mice with *B. microti*

The group of 20 BALB/c mice was injected with 150 µl of *B. microti* positive murine blood (parasitemia ~50 %). Control group of 20 BALB/c mice was injected with uninfected murine blood. Parasitemia of mice from experimental group was counted from sampled blood smears for 15 days post blood injection. On the 30th day sera were collected from 5 mice both from experimental and control group. Next, 5 mice from experimental group were re-infected 30 days post first infection (30 DPI). Parasitemia was counted and sera collected again. Same procedure was done with the next two groups of 5 mice which were re-infected 60 and 90 days post first infection (60 and 90 DPI). Mice from control group were infected with *B. microti* simultaneously as mice from experimental group and monitored the same way (Fig. 9).

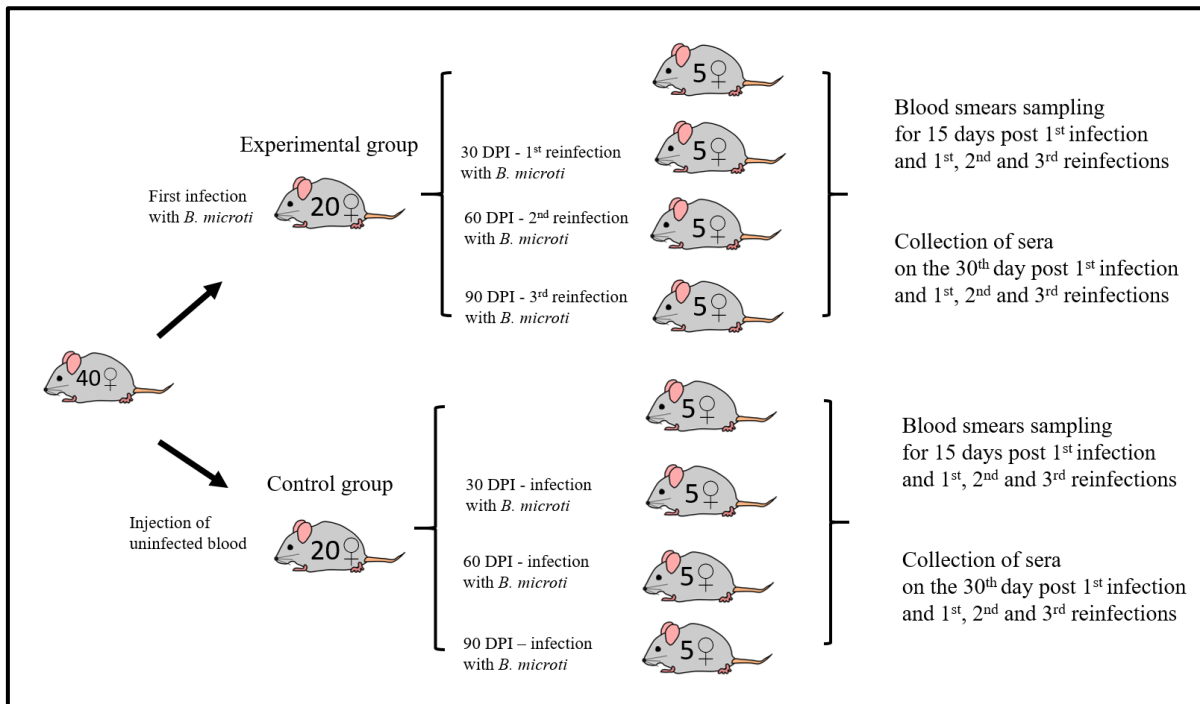


Figure 9: Experimental design of the repeated infections with *B. microti*. 20 mice were infected with *B. microti*, 20 mice were injected with uninfected blood as a control. Mice from experimental group were subjected to re-infections 30, 60 and 90 days post first infection. Progression of the infection was monitored using blood smear sampling. Smear was stained using DiffQuik staining set and parasitemia was calculated as percentage of infected erythrocytes per 1000 of erythrocytes for 15 days post re-infection. On the 30th day post first infection or re-infection sera were collected. Mice in control group were infected at the same timepoints as mice from experimental group were re-infected. DPI = days post-infection.

Collected murine sera were used in western blot analysis with AMA-1 recombinant protein. Western blot was conducted as described in chapter 3. 13. Murine sera and Anti-mouse IgG-peroxidase secondary antibody (Sigma-Aldrich, USA) were diluted by 1:100 and 1:2000, respectively, in 1% non-fat skimmed milk in 1 × PBS-T.

Nested PCR for validation of *B. microti* presence in murine blood 30 days post-infection was conducted as two separate PCR reactions using IR270, IR275 and IR272, IR273 primers. Both reactions proceeded as a standard PCR (Table 1) except for the volume of the template in the second reaction which was 1 µl. The volume of 25 µl reaction was adjusted with nuclease-free water.

4. Results

4.1. *B. microti* infection in mice and growth curve monitoring

The course of *B. microti* infection in mice was determined by daily examination of 15 mice = the control mice in the experiment - Evaluation of immunogenicity of *B. microti* AMA-1 protein in BALB/c mice (see 3. 15. and 4. 7.). The growth curve was divided into two phases (Fig. 10; A). The acute phase was characterized by rapid multiplication of the parasite. The infection progressed asynchronously. Therefore, we could determine both ring-like shaped trophozoites and amoeboid merozoites (Fig. 10; C). On the 6th day post-infection (6DPI) parasitemia reached the maximum ($44 \pm 2.8\%$). The lysis of infected erythrocytes caused the change in the ratio of red and white blood cells. Increased number of white blood cells indicated the development of immune response against the parasite. Additionally, a higher proportion of reticulocytes implied stimulation of hematopoiesis. The decline phase of infection lasted from 7th DPI to 15th DPI and was characterized by decreasing parasitemia up to $0.6 \pm 0.2\%$. Both host immune response and an increasing number of reticulocytes, within which the parasite could not multiply, caused that the mice eventually reached a complete recovery from the infection. It was proven by the examination of stained blood smears on 30th DPI where the parasite was not microscopically detected. However, using nested PCR, the persistence of *B. microti* in mice even 30 days post-infection was confirmed (Fig. 10; B).

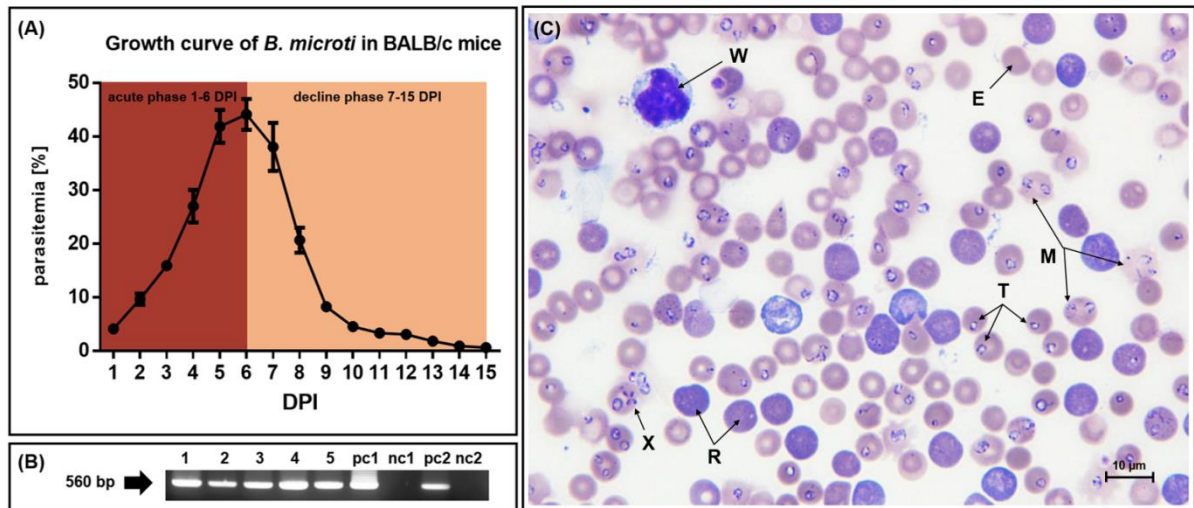


Figure 10: Characterization of *B. microti* infection in mice. (A) Parasite growth curve; parasitemia per 1000 erythrocytes was monitored for 15 DPI using blood smears stained by Diff-Quik Stain set. Results represent means of fifteen mice, error bars indicate standard error of mean. DPI = days post-infection. (B) Nested PCR; detection of *B. microti* DNA in the blood of mice on the 30th DPI; 1-5 = individual experimental mice, pc1 and nc1 = positive and negative control which went through both PCR rounds, pc2 and nc2 = positive and negative control which went through only second PCR round. (C) Blood smear of infected mouse in the peak of infection (6th DPI); M = merozoites, T = trophozoites, X = tetrad of merozoites, R = reticulocytes, E = mature erythrocytes, W = white blood cell.

4.2. Absolute quantification of *B. microti* in the gut and salivary glands of the ticks

The absolute quantification was performed as a number of *B. microti* (*ama-1* gene copies) per 10^3 tick genomes (*ferritin2* gene copies). Although nymphs were fed on mice with either increasing or decreasing levels of parasitemia, numbers of *B. microti* in the gut of 10 individual nymphs do not importantly differ. The changes of parasite numbers in the progression of tick feeding follow highly similar dynamics regardless of the acute or decline phase of mice infection. On 1DPA, the number of parasites in the gut ranged from 10^1 to 4.8×10^2 . On 2DPA, the number $4.8 \times$ dropped in comparison to the number of parasites on 1DPA. One of the ticks probably fed faster because the number of parasites went beyond the average value. On 3DPA, contrastingly, the number elevated by three orders in comparison to 1DPA. On 6DPD, *B. microti* still persisted in the tick gut. The number ranged from 2.4×10^2 to 18.7×10^3 (Fig. 11; A, B).

Surprisingly, *B. microti* presence was detected in the salivary glands already after 24 hours (1DPA). On average, 1.3×10^3 parasites were identified in the tissue. However, on 2DPA, the number slightly decreased. The average number determined was 3.7×10^2 . On 3DPA, the number of *B. microti* in salivary glands of nymphs fed in the acute phase ranged from 5.2×10^2 to 3.9×10^3 . Fewer parasites were identified in nymphs fed in the decline phase. The number ranged from 23 to 5.8×10^2 . On 6DPD, *B. microti* could be detected in the tissue. However, the numbers varied in the nymphs fed in the acute phase and the decline phase. Observed average numbers were 55 and 6.3×10^2 , respectively (Fig. 11; C, D).

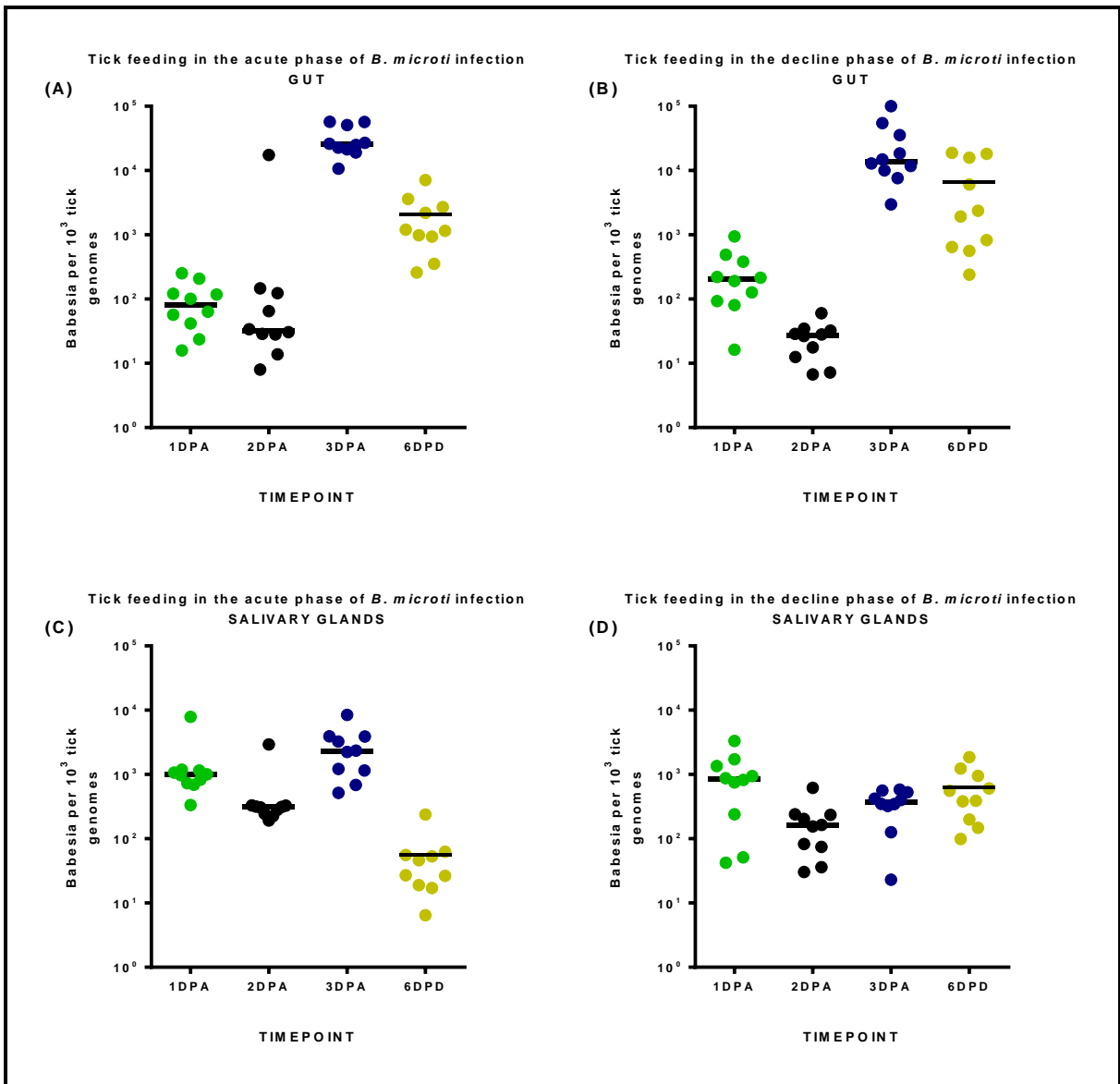


Figure 11: Absolute quantification of *B. microti* in the gut (A, B) and salivary glands (C, D) of *I. ricinus* nymphs fed on mice in different phases of parasite growth curve. Tick started feeding on infected mice either on 1st day post mice infection (acute phase of infection; A, C) or 6th day post mice infection (decline phase; B, D). Number of *B. microti* in the gut and the salivary glands was measured in on 24h (1DPA), 48h (2DPA), fully engorged nymphs (3DPA) and 6 days after tick detachment (6DPD). Each dot represents a number of *B. microti ama-1* gene copies per 10^3 tick genomes (*ferritin2* gene copies). DPA = day post tick attachment, DPD = day post tick detachment.

4.3. Relative expression of *ama-1* gene

4.3.1. Relative expression of *ama-1* gene in the murine blood positive for *B. microti*

Expression of *ama-1* gene was quantified in murine blood every second day during the acute and the decline phase of infection with *B. microti* (2DPI – 14DPI). Expression profile was complemented with the curve displaying the level of parasitemia in the murine blood in exactly same timepoints. Expression of the gene gradually rose which correlates with the multiplication of *B. microti* observed by a rapidly increasing number of merozoites and trophozoites in the host blood. Expression peaked on the 6th DPI when the highest parasitemia of 58% was detected (Fig. 12).

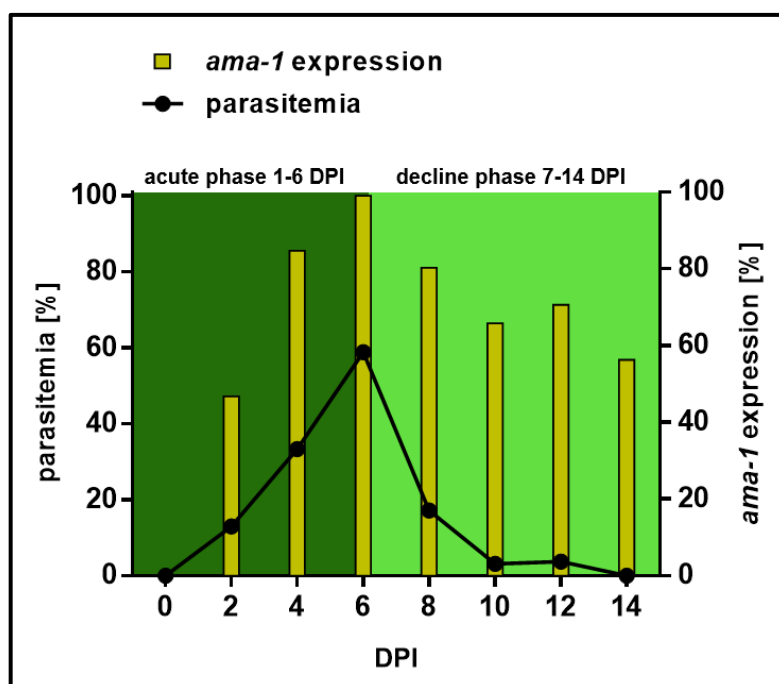


Figure 12: Relative expression of *ama-1* in murine blood throughout the progression of *B. microti* infection *in vivo*. Black curve represents the level of parasitemia during the infection of mouse with *B. microti*. Parasitemia per 1000 erythrocytes was monitored for 14 days (every second day) using blood smears stained by Diff-Quik Stain set. Yellow columns stand for the relative expression of *ama-1* gene measured in the specific timepoint. The relative expression of *B. microti ama-1* gene was normalized to *B. microti actin* gene, the highest expression in dataset was set at 100%. DPI = days post-infection.

Presented expression profile of *ama-1* gene served solely as an introductory experiment with no statistical importance. Therefore, only one repetition was conducted. We intended to verify the established method of *ama-1* expression detection and to get the corresponding result as Moitra et al. (2015) who confirmed the expression of AMA-1 in merozoites of *B. microti* (Moitra, Zheng et al. 2015).

4.3.2. Relative expression of *ama-1* gene in the gut and salivary glands of ticks feeding on mice in different phases of parasite growth curve.

Currently, there is the only evidence of *B. microti* AMA-1 protein expression in the vertebrate host. Therefore, we attempted to validate the expression also in stages of *B. microti* in the tick host. Since AMA-1 is a micronemal protein, we hypothesized its expression on the surface of invasive stages which possess these apical secretory organelles.

On 1DPA, relative expression of *ama-1* in the gut of nymphs fed on mice in the acute phase of infection was too low to reach the detection limit in the 1st trial but in the 2nd trial, we observed very low *ama-1* expression (2.2%). However, on 2DPA, steep growth of *ama-1* expression from 2.2 to 100% could be detected. On 3DPA, the expression sharply declined to 13.7% in the 1st trial and to 21.7% in the 2nd trial. Later, on 6DPD, none or only 2.6% expression was recorded (Fig. 13; A). A similar pattern of *ama-1* expression dynamics was observed also in ticks fed on mice in decline phase of parasitemia. Here, the *ama-1* expression in the gut of ticks fed in the decline phase (Fig. 13; B) was already detected after 24 hours of feeding since ticks started engorgement on mice with high parasitemia levels (~45%) in 1st trial but in the 2nd trial the *ama-1* expression was under the detection limit. The expression rose from 31% to 100% in the 1st trial and subsequently dropped sharply to 5% on 6DPD. In the 2nd trial, expression peaked on 2DPA and gradually decreased to 81% on 3DPA and to 22% on 6DPD. The peak infection in the 1st trial on 3DPA (Fig. 13; B) might be explained by the fact that nymphs could feed more slowly.

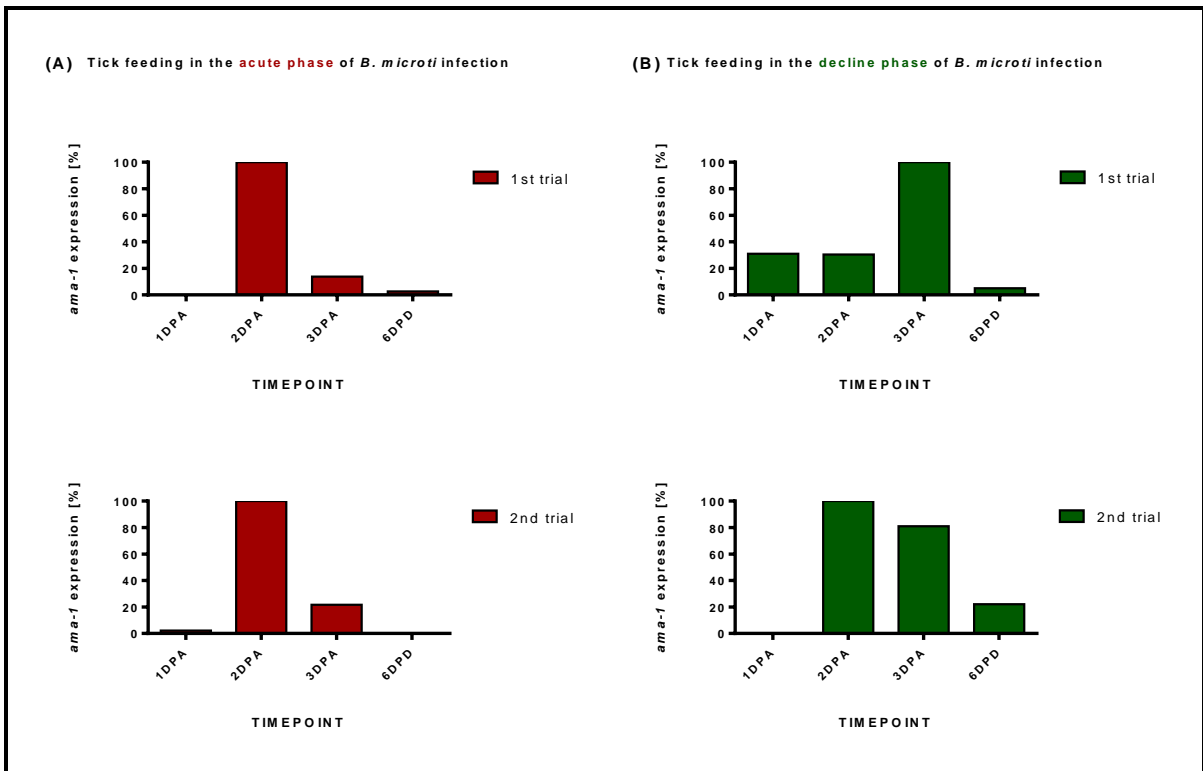


Figure 13: Relative expression of *B. microti ama-1* gene in the gut of *I. ricinus* nymphs fed on mice in different phases of parasite growth curve. Tick started feeding on infected mice either in the acute phase (A) or the decline phase of infection (B). Expression was measured on 24h fed nymphs (1DPA), 48h fed nymphs (2DPA), fully engorged nymphs (3DPA) and 6 days after tick detachment (6DPD). One of the columns in each timepoint represents for the gene expression measured in the pool of guts dissected from 10 nymphs, two separate biological trials were carried out. The relative expression of *B. microti ama-1* gene was normalized to *B. microti actin* gene, the highest expression in each dataset was set at 100%. DPA = days post tick attachment, DPD = days post tick detachment.

Relative expression of *ama-1* gene in salivary glands of nymphs fed on mice in the acute phase of infection could not be identified on 1DPA since the gene expression was below the detection limit. Conversely, the highest expression (100%) was observed on 2DPA in the 2nd trial. It gradually decreased to 66% (3DPA) and 8.4 % (6DPD) (Fig. 14; A). Results from the 1st trial could not be analysed as the *ama-1* expression has been detected only on 2DPA. Therefore, the analysis of *ama-1* expression in the course of tick feeding could not be proceeded. The relative expression of *ama-1* gene in the salivary glands of ticks fed on mice in the decline phase of infection (Fig. 14; B) was steadily increasing until it peaked after on 3DPA. Eventually, the expression went down on 6DPD. In the 1st trial, the *ama-1* expression ranged as follows: none, 18.3%, 100% and 24.7%. In the 2nd trial the expression ranged as follows: 2.4%, 29.5%, 100% and 29.5%.

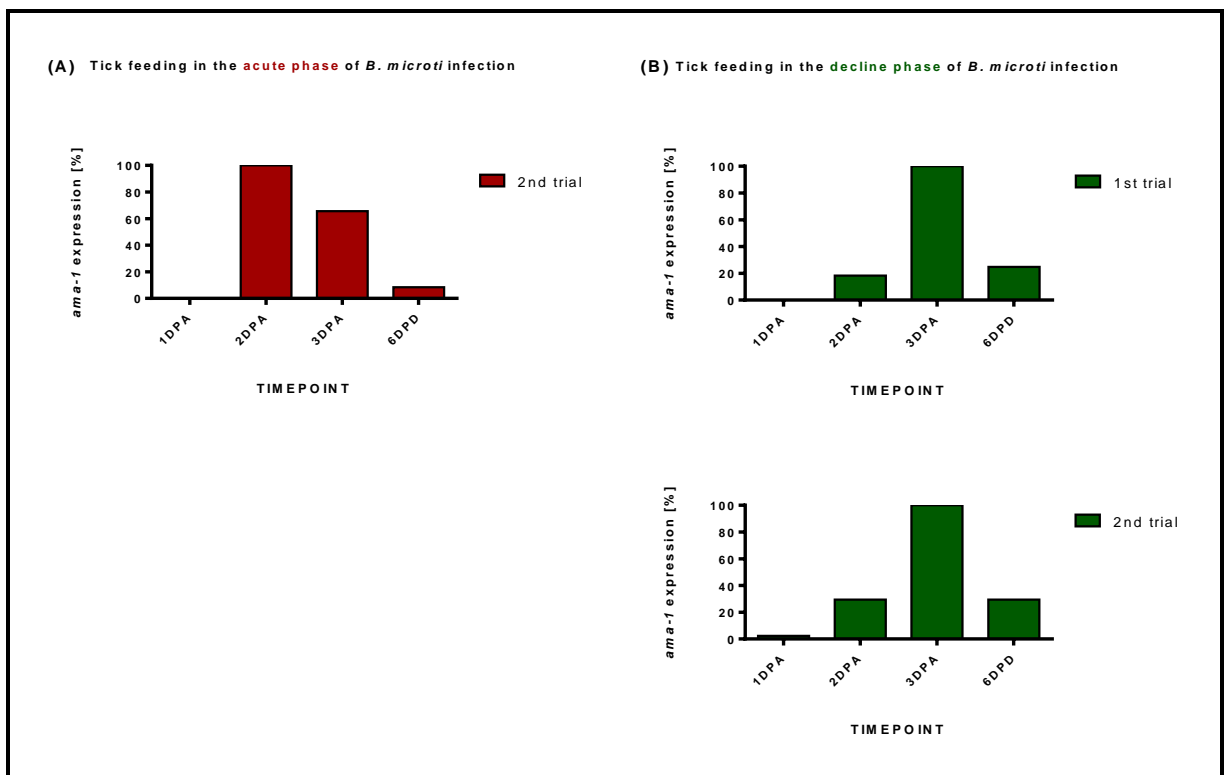


Figure 14: Relative expression of *B. microti ama-1* gene in the salivary glands of *I. ricinus* nymphs fed on mice with different levels of parasitemia. Tick started feeding on infected mice either in the acute phase (A) or the decline phase of infection (B). Expression was measured on 24h fed nymphs (1DPA), 48h fed nymphs (2DPA), fully engorged nymphs (3DPA) and 6 days after tick detachment (6DPD). One of the columns in each timepoint represents for the gene expression measured in the pool of salivary glands dissected from 10 nymphs, two separate biological trials were carried out. The relative expression of *B. microti ama-1* gene was normalized to *B. microti actin* gene, the highest expression in each dataset was set at 100%. DPA = days post tick attachment, DPD = days post tick detachment.

4.4. AMA-1 recombinant protein synthesis and antisera production

The amplified fragment of the selected part of *ama-1* gene (Fig. 15; A) was cloned into the vector. Colony PCR confirmed the presence of the inserted fragment of *ama-1* gene – the outer exposed region of the size of 650bp in four of 8 tested colonies (Fig 15; B). Verified by sequencing, sequence of inserted fragment was translated using an online ExPasy Translate Tool. A possible shift of open reading frame was excluded and the presence of His-Tag was confirmed (Fig. 16). Anti-His tag primary antibody used in the western blot analysis identified expression AMA-1 recombinant protein of the size of 29kDA (Fig. 17; A). Individual fractions of purified protein are visualized in figure 17; B. The production of rabbit antibodies anti-AMA-1 recombinant protein was confirmed by the western blot analysis using AMA-1 recombinant protein and immune rabbit serum (Fig. 17; C).

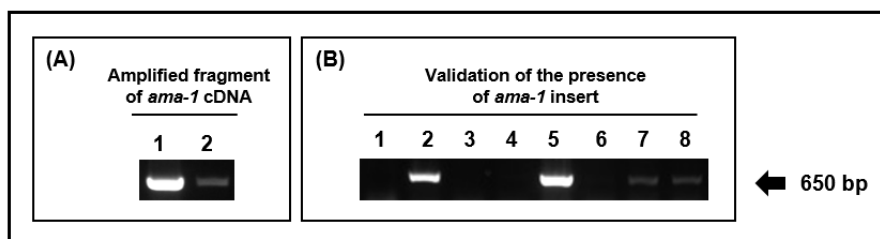


Figure 15: Cloning of *ama-1* gene fragment. (A; 1, 2) Amplified fragment of *ama-1* – 650 bp was cloned into the vector. (B) Colony PCR validated the presence of inserted sequence in the vector. Each number represents one tested colony.

```

1 atg cgg ggt tct cat cat cat cat cat cat ggt atg gct agc atg act ggt gga cag caa
1 M R G S H H H H H H G M A S M T G G Q Q
61 atg ggt cgg gat ctg tac gac gat gac gat aag gat cat ccc ttc acc act gcc aaa aca
21 M G R D L Y D D D D K D H P F T T A K T
121 ctg aaa gca tac gaa tat gac ggg gat gat ata ttc aac tgc gcc tcc tat gca agc gaa
41 L K A Y E Y D G D D I F N C A S Y A S E
181 ttg atg atg agt agt gac aga aag tct gat tac aaa tat cca ttt gcc ttt gat ttg aaa
61 L M M S S D R K S D Y K Y P F A F D L K
241 act aaa act tgc cac atc tta tac tct ccg ttg caa cta atc cag gga cct aag tat tgt
81 T K T C H I L Y S P L Q L I Q G P K Y C
301 gat aat gat gga aaa gtg gat agt ggt tcc agc agt atg cct tgt att aag ccc gtg aag
101 D N D G K V D S G S S S M P C I K P V K
361 gac atg agt caa gaa atg gtt tat gga tct tcc ttc att tac agg gac tgg aaa aat aaa
121 D M S Q E M V Y G S S F I Y R D W K N K
421 tgt ccc aat gcg gcg gtg gca gat gca att ttt ggt acc tgg aac ggc acg gct tgc gtt
141 C P N A A V A D A I F G T W N G T A C V
481 cca att cag aat agg aga tta ttc aag gct tct act cct gaa att tgc ggt caa ata gtg
161 P I Q N R R L F K A S T P E I C G Q I V
541 ttc aaa tat agt gca tcg gat gca ccg gaa aat tat gaa act aaa cgc agt gaa ggt tct
181 F K Y S A S D A P E N Y E T K R S E G S
601 aaa ttt gca aat gca atc tca tct ggt gac ctt ggt gca gtt gct aag att ata atg cct
201 K F A N A I S S G D L G A V A K I I M P
661 gtc aca aac tct cgc gcc cac cac tcc aag gga tgg ggc ttc aat tgg gcc aat tat gat
221 V T N S R A H H S K G W G F N W A N Y D
721 agg aat aag cgt gaa tgt ggc tta atc gat gag gtt cca aat tgt cta gtt ttc aag atg
241 R N K R E C G L I D E V P N C L V F K M
781 gga aac att gca tag
261 G N I A *

```

Figure 16: Nucleotide and amino acid sequence of AMA-1 recombinant protein. Grey background displays inserted sequence. His-tag is highlighted in yellow color.

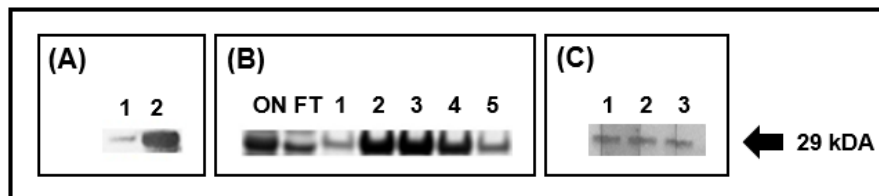


Figure 17: Expression and purification of AMA-1 recombinant protein. (A) Western blot with AMA-1 recombinant protein and anti-His tag antibody; cell lysate before (1) and after (2) induction of expression of recombinant protein by IPTG. (B) SDS-PAGE with AMA-1 purified recombinant protein; ON - cell lysate loaded on the column, FT - flow through of proteins which did not bind to the column, 1 – 5 - fractions of recombinant protein. (C) Western blot with purified recombinant protein and rabbit immune serum (dilution of the serum: 1 – 1:1000, 2 – 1:2000, 3 – 1:5000).

4.5. Anti-AMA-1 antibodies detected *B. microti* in the murine blood

Generated antibodies against AMA-1 were successfully used for visualization of blood stages of *B. microti* (Fig. 18; A). The controls using a non-immune serum (Fig. 18; B) and only secondary antibody (Fig. 18; C) confirmed the specificity of generated antibodies. The mispecificity of antibodies was excluded using IFAT (immunofluorescence antibody test) on negative murine blood (Fig. 18; D).

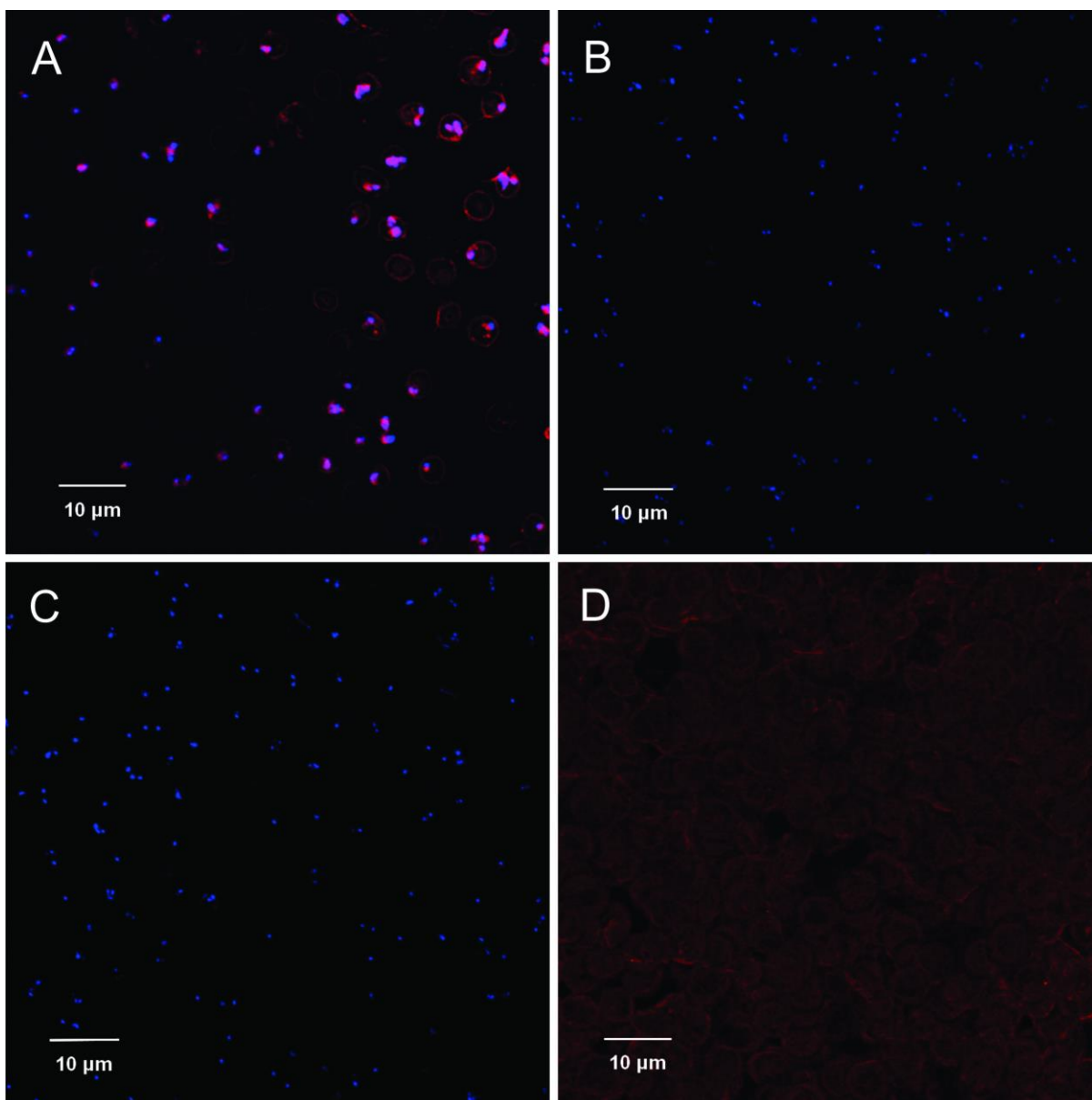


Figure 18: Immunodetection of *B. microti* in the blood of infected mouse. Blood samples were taken from the tail of BALB/c mouse in the peak of infection (6DPI). Prepared blood smears underwent the staining procedure by (A) rabbit-anti-AMA-1 serum and secondary antibody Alexa Fluor[®] 647 (red signal). Nuclei of cells (blue signal) were stained by DAPI (4', 6-diamidin-2-fenylindol). (B) Nonimmune rabbit serum and (C) only secondary antibody applied served as controls. (D) Blood smear with negative murine blood excluded mispecificity of the reaction. Stained blood smears were examined by confocal microscope Olympus FW1000. Photos were processed in Fluoview software (FV10-ASW, version 4.2). DPI = days post-infection.

4.6. Immunodetection of *B. microti* in the gut of fully fed nymph

We immunodetected *B. microti* also in the gut lumen of the infected nymph with anti-AMA-1 antibody (Fig. 19; C). However, we did not identify any signal in stages invading the tick gut wall (Fig. 19; A, B). This unexpected result is further discussed in chapter 5.

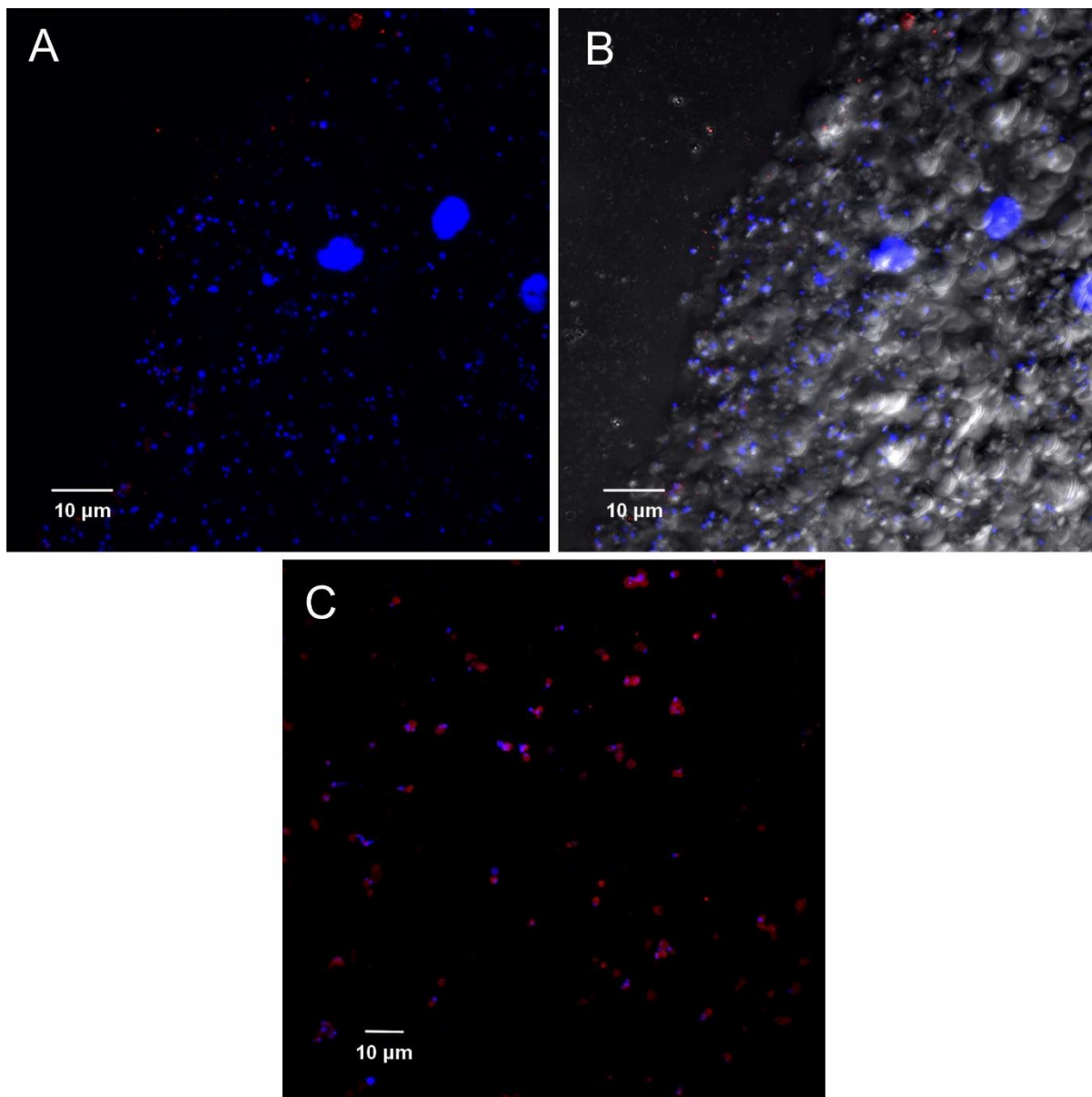


Figure 19: Immunodetection of *B. microti* in the gut of infected nymph. Gut tissue and its content were obtained by dissection of fully engorged infected *I. ricinus* nymph which fed on *B. microti* positive mouse in the decline phase of infection. Prepared blood smears underwent the staining procedure by rabbit-anti-AMA-1 serum and secondary antibody Alexa Fluor[®]647. Nuclei of cells (blue signal) were stained by DAPI. (A, B) *B. microti* in the tick gut epithelial cells without and with Nomarski differential interference contrast. (C) *B. microti* within the gut content of fully engorged nymph.

4.7. Evaluation of immunogenicity of *B. microti* AMA-1 protein in BALB/c mice

Infection with *B. microti* was already confirmed to be self-limiting in BALB/c mice (Igarashi et al. 1999). Therefore, we set up the re-infection experiment to subsequently examine whether the mice can generate protective immunity and whether the humoral immune response is targeted against AMA-1 surface antigen.

4.7.1. Primary infection protects mice against re-infection with *B. microti*

The experimental mice subjected to *B. microti* re-infection 30 days after the first challenge displayed resistance to the parasite; the parasites on the blood smears could be detected only until second day post re-infection and parasitemia did not exceed 1% (Fig. 20; A). Unexpectedly, on the 14th day, parasite was detected in three mice out of five, which could indicate a possible progression of relapse. However, this phenomenon was not subjected to further studies. The experimental mice subjected to *B. microti* re-infection 60 days after the first challenge also demonstrated resistance to the parasite. Parasitemia in the blood of mice reached 1.2% maximum. No parasite could be detected on the 5th day post re-infection (Fig. 20; C). The last group of experimental mice, which was re-infected 90 days after the first challenge, manifested also the resistance to *B. microti*; the parasites on the blood smears could be detected the first day in all mice. From the second until the fifth day parasite was detected only in two mice out of four and parasitemia did not exceed 5% (Fig. 20; E). In contrast to mice subjected to re-infection, control groups demonstrated the standard progression of infection (Fig. 20; B, D, F).

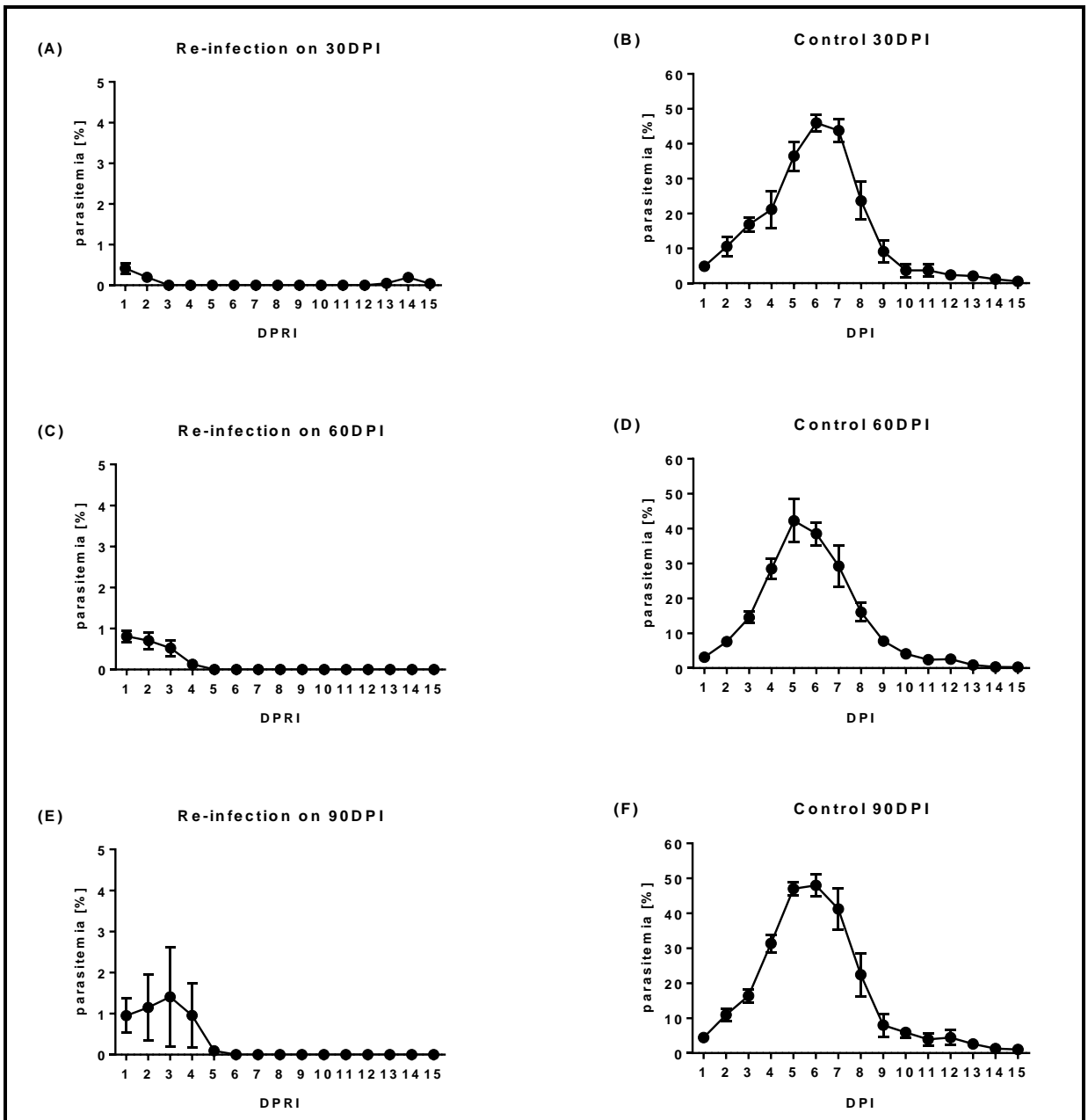


Figure 20: Repeated challenges of BALB/c mice to *B. microti* infection. Second challenges were performed (A) 30 days after primary infection (30 DPI), (C) on 60 DPI and (E) on 90 DPI. Similarly, the control mice were subjected to *B. microti* challenge after injection of non-infected blood on (B) 30DPI, (D) 60DPI, (F) 90DPI. Parasitemia was monitored daily for 15 days after the challenge using blood smears stained by Diff-Quik Stain set and derived as a number of parasitized erythrocytes per 1000 erythrocytes. DPI = days post-infection.

4.7.2. Infected mice generate antibodies targeting AMA-1 protein

The specific antibodies against AMA-1 were detected in sera collected from mice subjected to re-infection challenges (Fig. 21). More than half of mice from the re-infection experiment exhibited positive reaction. This could imply that AMA-1 is probably one of the surface antigens against which the vertebrate host develops the immune response.

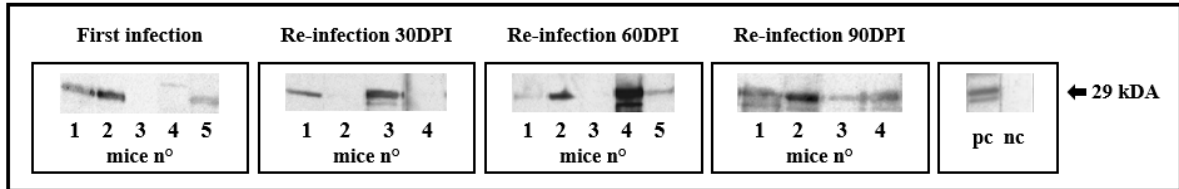


Figure 21: Detection of specific AMA-1 antibodies in mouse sera. The analysis was performed by western blot with AMA-1 recombinant protein and mouse sera collected 30th day after either first infection or re-infection performed in different timepoints (30, 60 or 90 DPI). pc = positive control (murine blood positive for *B. microti* and mixture of mouse sera collected from infected mice); nc = negative control (recombinant protein and mixture of sera from five samples of negative murine blood). DPI = days post-infection.

4.8. Relative expression of *ccp2* gene

Since the expression of AMA-1 in *Babesia* sexual stages is speculative, we have decided to use specific markers for parasite sexual stages: *ccp* genes / CCp proteins. Hence, we examined *ccp2* gene expression, so far the only described CCp protein for *B. microti*.

4.8.1. Relative expression of *ccp2* gene in the murine blood infected with *B. microti*

Expression of *ccp2* gene was quantified in murine blood every second day during the acute and the decline phase of infection with *B. microti* (2DPI – 14DPI). Expression profile was complemented with the curve displaying a level of parasitemia in murine blood in the exactly same timepoints. Expression of the gene manifested fluctuating character. It firstly followed the upward trend of parasitemia. However, in the peak of infection, it dropped to 61% and steadily fell to 32% until the 8th day post-infection. On the 10th day post-infection it sharply went up to 100% and gradually decreased to 40% until 14DPI timepoint (Fig. 22). However, it is necessary to admit that this analysis was not performed in biological replicates and needs to be repeated.

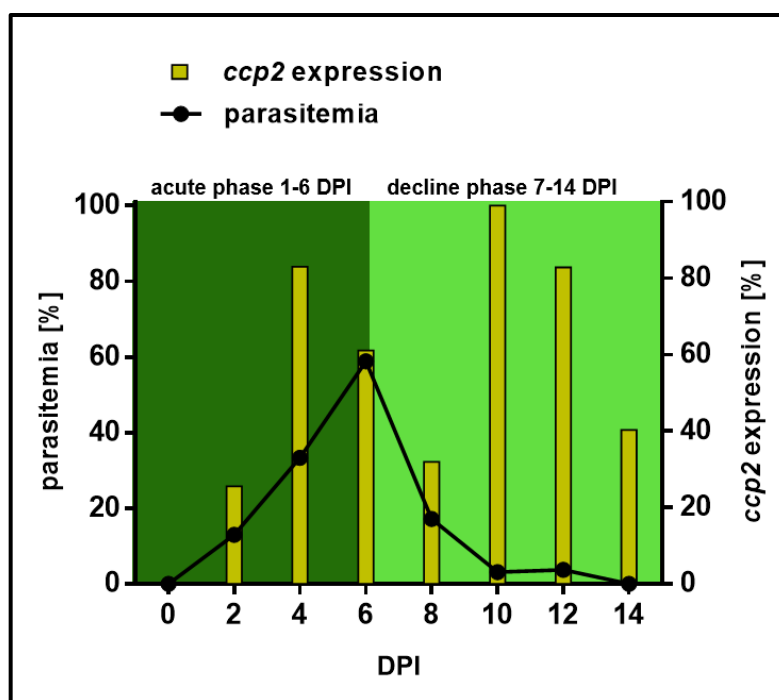


Figure 22: Relative expression of *ccp2* in murine blood throughout the progression of *B. microti* infection *in vivo*. Black curve represents the level of parasitemia during the infection of mouse with *B. microti*. Parasitemia per 1000 erythrocytes was monitored for 14 days (every second day) using blood smears stained by Diff-Quik Stain set. Yellow columns stand for relative expression of *ccp2* measured in a specific timepoint. The relative expression of *B. microti ccp2* was normalized to *B. microti actin* gene, the highest expression in dataset was set at 100%. DPI = days post-infection.

4.8.2. Relative expression of *ccp2* in the gut and salivary glands of ticks feeding on mice with different level of parasitemia

The highest expression of *ccp2* was detected on 3DPA in the gut of nymphs fed on mice in the acute phase of infection. Later, on 6DPD, the expression slightly dropped to 74%. In previous timepoints, the expression was probably too low to reach the detection limit (Fig. 23; A). In the 2nd trial, the *ccp2* expression has been detected only on 3DPA. Therefore, the analysis of *ccp2* expression in the course of tick feeding could not be proceeded in the second trial. However, the Cp values of *actin* gene did not differ from those obtained in the first trial.

Contrastingly, the expression of the *ccp2* gene in the gut of ticks fed on mice in the decline phase was already detected on 1DPA (18.3%). The expression gradually rose and on 6DPD it ranged from 60 to 87% (1st and 2nd trial). Earlier expression of *ccp2* in the first trial (Fig. 23; B) is probably caused by the fact that nymphs were feeding faster.

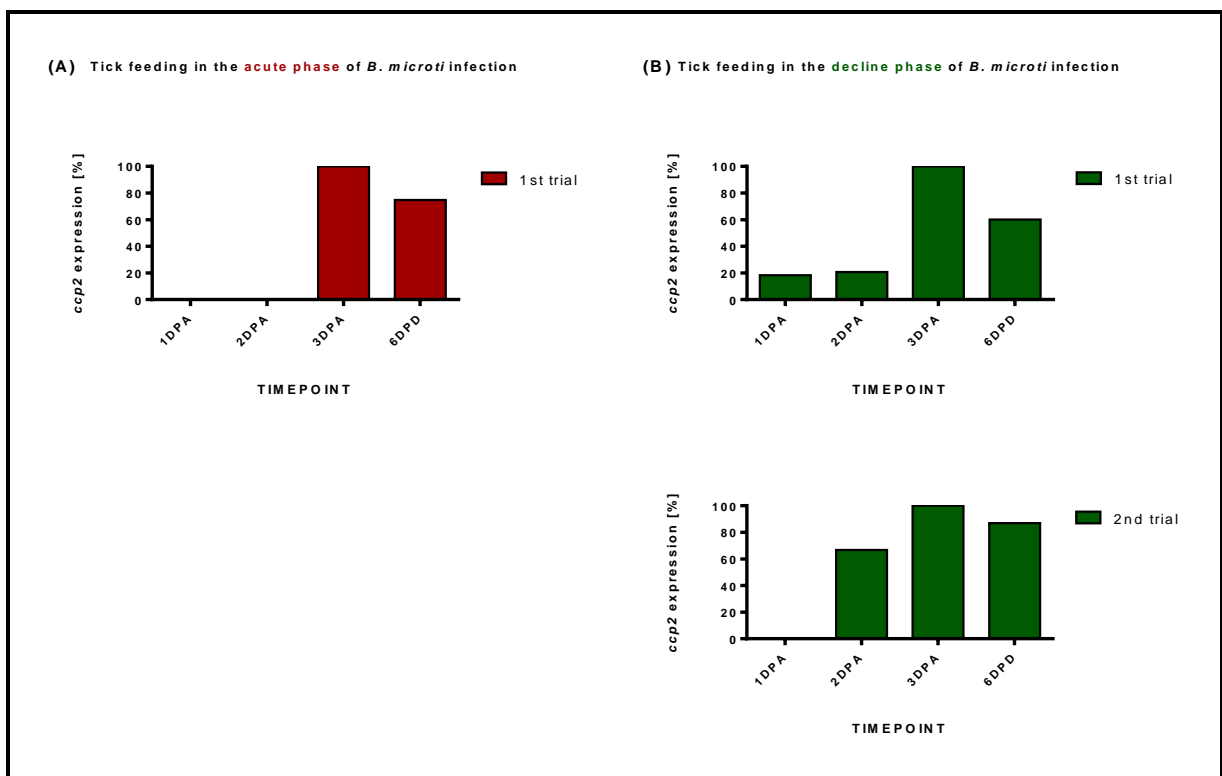


Figure 23: Relative expression of *B. microti ccp2* gene in the gut of *I. ricinus* nymphs fed on mice in different phases of parasite growth curve. Tick started feeding on infected mice either in the acute phase (A) or the decline phase of infection (B). Expression was measured on 24h fed nymphs (1DPA), 48h fed nymphs (2DPA), fully engorged nymphs (3DPA) and 6 days after tick detachment (6DPD). One of the columns in each timepoint represents for the gene expression measured in the pool of guts dissected from 10 nymphs, two separate biological trials were carried out. The relative expression of *B. microti ccp2* gene was normalized to *B. microti actin* gene, the highest expression in each dataset was set at 100%. DPA = days post tick attachment, DPD = days post tick detachment.

Relative expression of *ccp2* in salivary glands of nymphs fed on mice in the acute phase of infection was firstly identified on 3DPA in both trials (6.6% and 39.6%). Expression peaked (100%) on 6DPD (Fig. 24; A). Expression in salivary glands of nymphs fed on mice in the decline phase of infection manifested fluctuating character in the 1st trial (77.6%, 20.3% and 100%). Results from the 2nd trial could not be analyzed (Fig. 24; B). The undetectable *ccp2* expression could be a result of either too low concentration or possible degradation of RNA.

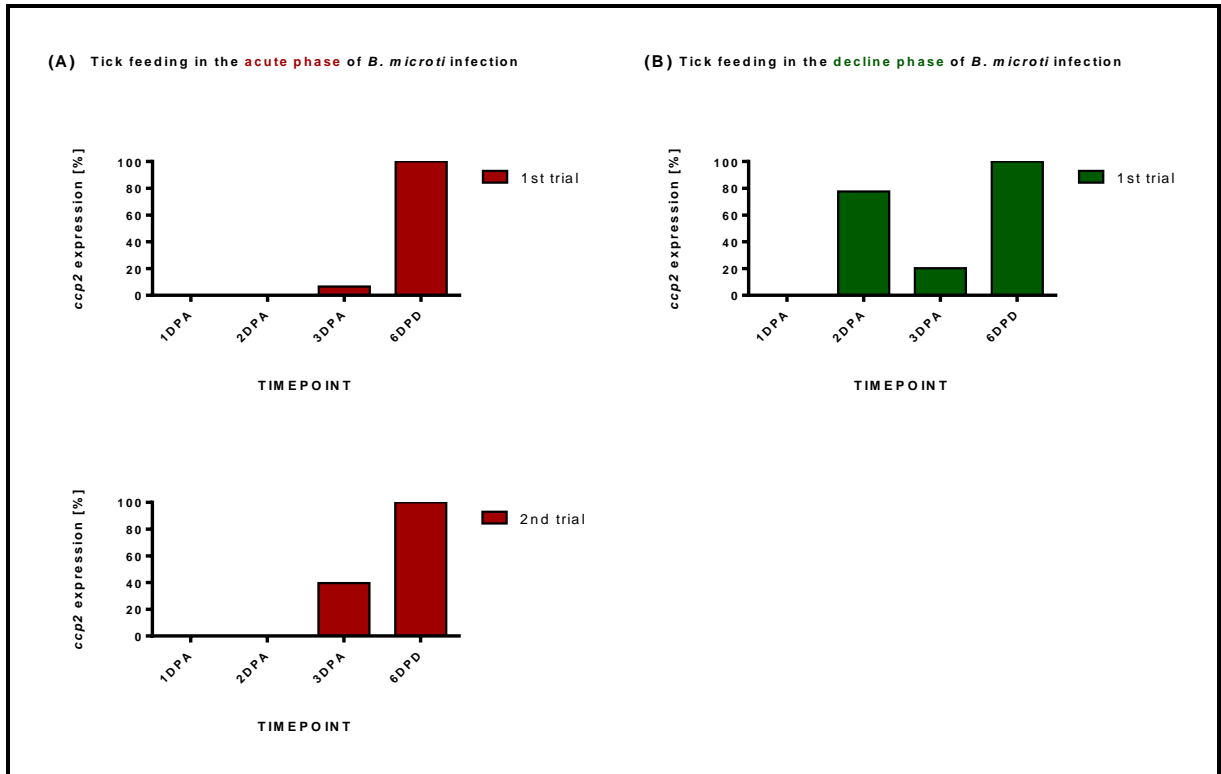


Figure 24: Relative expression of *B. microti ccp2* gene in the salivary glands of *I. ricinus* nymphs fed on mice with different levels of parasitemia. Tick started feeding on infected mice either in the acute phase (A) or the decline phase of infection (B). Expression was measured on 24h fed nymphs (1DPA), 48h fed nymphs (2DPA), fully engorged nymphs (3DPA) and 6 days after tick detachment (6DPD). One of the columns in each timepoint represents for the gene expression measured in the pool of salivary glands dissected from 10 nymphs, two separate biological trials were carried out. The relative expression of *B. microti ccp2* gene was normalized to *B. microti actin* gene, the highest expression in each dataset was set at 100%. DPA = days post tick attachment, DPD = days post tick detachment.

4.9. Expression and purification of CCp2 recombinant protein

The presence of the inserted fragment (Fig. 25; A) was validated by PCR (Fig 25; B) in all tested colonies. Verified by sequencing, the sequence of inserted fragment was translated using an online ExPasy Translate Tool. A possible shift of open reading frame was excluded and the presence of His-Tag was confirmed (Fig. 26). Anti-His-tag primary antibody used in the western blot analysis identified expression of CCp2 recombinant protein of the size of 28kDA (Fig. 27; A). Individual fractions of purified protein are visualized in fig. 27; B. The production of rabbit antibodies anti-CCp2 recombinant protein will be prepared by immunization of the rabbit in the future.

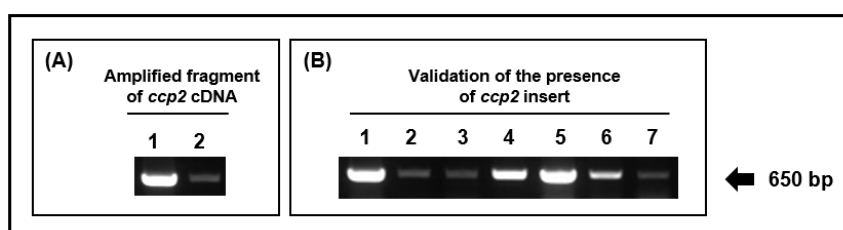


Figure 25: Cloning of *ccp2* gene fragment. (A; 1, 2) Amplified fragment of *ccp2* – 650 bp was cloned into the vector. (B) Colony PCR validated the presence of inserted sequence in the vector. Each number represents one tested colony.

1	atg	cg	gg	tct	cat	cat	cat	cat	cat	cat	ggt	atg	gct	agc	atg	act	ggt	gga	cag	caa
1	M	R	G	S	H	H	H	H	H	H	G	M	A	S	M	T	G	G	Q	Q
61	atg	ggt	cg	gat	ctg	tac	gac	gat	gac	gat	aag	gat	cat	ccc	ttc	acc	ccc	gtg	gca	ttt
21	M	G	R	D	L	Y	D	D	D	D	K	D	H	P	F	T	P	V	A	F
121	ata	tca	gat	gga	aaa	ttt	aaa	tca	tta	gac	ctt	aat	aca	gac	tcc	act	gag	gca	ctt	gaa
41	I	S	D	G	K	F	K	S	L	D	L	N	T	D	S	T	E	A	L	E
181	aat	ttg	ggt	aat	cat	aat	gat	ggt	gat	aac	acg	ata	gct	gtg	tcc	cgt	gat	gct	atc	atg
61	N	L	V	N	H	N	D	G	D	N	T	I	A	V	S	R	D	A	I	M
241	ggt	atc	gat	tct	acc	act	aaa	gaa	atg	gcc	gga	att	ata	tgc	ggc	ttc	tat	ggg	caa	cca
81	G	I	D	S	T	T	K	E	M	A	G	I	I	C	G	F	Y	G	Q	P
301	atg	aaa	tcc	ata	gat	tgc	gtc	acg	acg	atg	aag	agt	ctc	agt	cac	aca	cta	ggc	aat	gaa
101	M	K	S	I	D	C	V	T	T	M	K	S	L	S	H	T	L	G	N	E
361	tac	ctg	ttc	tct	tgt	cca	tct	gat	tgt	cca	aag	aaa	ttg	gat	aca	gat	aaa	ttt	agg	cta
121	Y	L	F	S	C	P	S	D	C	P	K	K	L	D	T	D	K	F	R	L
421	gta	ggt	ggg	ttc	gag	gcc	cta	act	aca	aac	act	ggt	ggt	cat	aaa	gct	ttc	gtg	ttc	acg
141	V	G	G	F	E	A	L	T	T	N	T	G	V	H	K	A	F	V	F	T
481	atg	gac	agt	ccg	ttg	tgc	ctt	gcg	gct	gct	ggt	aat	ggc	agc	agg	tac	ata	agg	act	aaa
161	M	D	S	P	L	C	L	A	A	A	V	N	G	S	R	Y	I	R	T	K
541	ggt	att	cag	ggg	ctg	gaa	agt	tat	gga	gga	ttc	gtc	gct	aat	ggc	ggt	gtg	gct	gaa	gcg
181	V	I	Q	G	L	E	S	Y	G	G	F	V	A	N	G	V	V	A	E	A
601	gta	gag	ggc	caa	aga	ggg	gaa	ttt	gcc	gtg	gaa	ata	ttg	ggc	cta	tgt	agc	aac	agc	aaa
201	V	E	G	Q	R	G	E	F	A	V	E	I	L	G	L	C	S	N	S	K
661	tcg	gat	aac	att	ctt	agt	agt	gga	aac	act	aca	att	ggc	aaa	aca	aaa	att	agt	gga	aca
221	S	D	N	I	L	S	S	G	N	T	T	I	G	K	T	K	I	S	G	T
721	agt	gaa	ata	cct	aag	gct	gcc	ccc	agg	aag	gat	act	ggc	atc	gga	tag				
241	S	E	I	P	K	A	A	P	R	K	D	T	G	I	G	*				

Figure 26: Nucleotide and amino acid sequence of CCp2 recombinant protein. Grey background displays inserted sequence. His-tag is highlighted in yellow color.

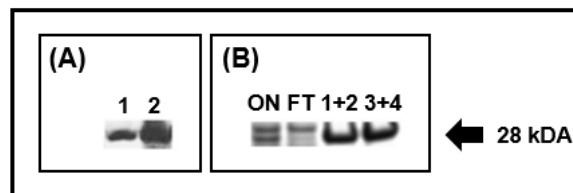


Figure 27: Expression and purification of CCp2 recombinant protein. (A) Western blot with CCp2 recombinant protein and anti-His tag antibody; 1, 2 – cell lysate before and after induction of expression of recombinant proteins by IPTG, respectively. (B) SDS-PAGE with CCp2 purified recombinant protein; ON - cell lysate loaded on the column, FT - flow through of proteins which did not bind to the column, 1 – 4 - fractions of recombinant protein.

5. Discussion

In this work, we intended to select and examine surface markers of *B. microti* which would function reliably in the detection of different stages of the parasite within the tick host. These markers could be further used both for studying the development of the parasite in the tick host and for elucidating possible interactions between the parasite and the immune system of the tick. One of the selected markers was AMA-1; a transmembrane protein which is involved in the process of host cell invasion. AMA-1 is transported from micronemes of the parasite and together with a group of RON proteins form a complex known as moving junction (Besteiro et al. 2011). Expression of the protein was previously confirmed in invasive stages of *B. microti* which asexually multiply in the host blood (Moitra et al. 2015). However, blood stages (merozoites) are not the only invasive stages which acquire apical complex organelles (Rudzinska and Trager 1977). The apical structures can be found also in kinetes and sporozoites which develop in the tick host (Karakashian et al. 1983; Karakashian et al. 1986). Therefore, hypothetically, AMA-1 could be also localized in these stages and play a role both in the invasion of internal tick tissues and in the invasion of erythrocytes by sporozoites during the tick bite. Up to know, no knowledge about AMA-1 expression in the aforementioned intra-tick stages exists.

Insight into the development and ama-1 expression of B. microti in the blood of the vertebrate host

Firstly, we observed the duration of the parasite development in the bloodstream of mice and derived the parasite growth curve which was divided into acute and decline phase (Fig. 10; A). Subsequently, we validated *ama-1* expression in the blood of BALB/c mice. The increasing expression of *ama-1* correlated with the upward trend of the parasite growth curve. The elevation of the expression was most probably due to a rapid multiplication of asexual stages which are characteristic of AMA-1 expression (Moitra et al. 2015) (Fig. 12).

Screening of ama-1 expression and the presence of the parasite in the tick host tissues

In several publications, Rudzinska and her colleague Karakashian provided detailed research on the progression of the *B. microti* in the tissues of *I. scapularis* and especially on the morphology of the single intra-tick stages (Rudzinska et al. 1979; Karakashian et al. 1986). Nevertheless, limited information is still presented about the life cycle within the tick tissues with respect to the time span. We intended to observe the potential dynamics of *ama-1* gene expression related to the number of parasites present in the tick tissues. We initially examined the absolute number of parasites and relative gene expression in the nymphs fed

on mice in the acute phase of infection. Since the parasitemia was ~5% at the beginning of tick feeding and gradually increased to ~30% by the end of the feeding (acute phase), we consequently focused also on the nymphs which started feeding when the parasitemia was already ~42% and gradually decreased to ~18% by the end of the feeding (decline phase).

Regardless the nymphs were feeding on mice with different levels of parasitemia, the numbers of *B. microti* in the gut of nymphs were approximately equal. On the first days of tick feeding, the parasite could be observed in the gut in relatively low numbers but on the third day, the numbers were three times higher which might suggest intensive reproduction of the parasite. Six days post-repletion, the parasite still persisted in the gut but in lower numbers (Fig. 11). On the first day, we did not identify *ama-1* expression in the gut of the nymphs fed in the acute phase (Fig. 13). It is likely that the gene was expressed but very likely the expression was too low to reach the detection limit of the method. Therefore, the analysis could not be evaluated despite the fact that *actin* (housekeeping gene) was expressed. On the contrary, we detected the low expression of *ama-1* on the first day in the nymphs feeding during the decline phase. This occurrence can be explained by the fact that ticks were feeding on considerably higher parasitized blood. Expression of *ama-1* very likely indicates the presence of merozoites in the gut lumen. Throughout the next days of tick feeding expression of *ama-1* gene rose and later in fully fed ticks as well as six days post-repletion decreased. To sum up, the dynamics of *ama-1* expression was analogous in all four trials regardless of tick feeding in acute or decline phase.

The highest expression of *ama-1* was detected on the second day while the most parasites were found on the third day in the tick gut. The lower *ama-1* expression on the third day implies that the merozoites are not probably so abundant in the gut lumen, while the high absolute number of the parasites very likely indicates ongoing intense multiplication of *B. microti*. However, we can only speculate on whether the absolute numbers reflect either generation of gametes in the gut lumen or massive division of zygotes in the gut wall and kinetes production. Such reproduction could be initiated already on the first days of tick feeding.

Six days post-repletion, merozoites can probably be no longer found in the gut lumen and if so, in very low numbers. This notion is supported by previous research when DNA from murine blood was not detected in the tick gut on 6DPD. The occurrence of the asexual stages is therefore unlikely (Jalovecka 2017). This assumption would correlate with the decreased *ama-1* expression. If merozoites cannot be found in the lumen on 6DPD and *ama-1* is still expressed albeit little in that timepoint in the gut, it is possible that some of the stages involved

in intra-gut reproduction can express the gene. Our microscopy results (discussed further, Fig. 19) suggest that very likely the expression of *ama-1* gene is not associated with kinetes. However, the previous research confirmed the *ama-1* expression in gametes of *E. tenella* (Jiang et al. 2012). The fact that the gametes persist in the lumen is supported also by the *ccp2* expression analysis. Therefore, the *ama-1* gene expression might correspond with the presence of gametes but this hypothesis needs the verification.

Unexpectedly, we identified the parasite in salivary glands already on the first day of tick feeding (Fig. 11). *B. microti* was present in the tissue throughout the whole period of tick feeding and also six days post-repletion. Expression of *ama-1* was also detected (Fig. 14). Initially, it displayed an increasing trend. Eventually, it decreased six days post-repletion. It is difficult to explain the phenomenon of the parasite presence as well as *ama-1* expression in this tissue. Since it is very probable that AMA-1 is expressed on sporozoites, invasive blood stages, the detection of *ama-1* mRNA might suggest that this gene expression is initiated already in the early phases of sporogony. Decrease of the expression on the 6th day post-repletion would imply the beginning of a dormant stage of the parasite. Assumption of AMA-1 expression in *B. microti* sporozoites would be in line with the results of the protein identification in sporozoites of *P. falciparum* (Silvie, Franetich et al. 2004) and *E. tenella* (Jiang et al. 2012).

As for the unexpected presence of *B. microti* parasites in tick salivary glands on the first day of tick feeding, it is possible that kinetes invading the tissue are already developed at that time. However, this circumstance is speculative. The only evidence of the development of *B. microti* gametes and zygotes has been provided by Rudzinska in the study with *I. scapularis* larvae (Rudzinska et al. 1979; Rudzinska et al. 1982). In the electron microscopy sections, they found gametes 18 – 20 hours post-repletion in the tick gut lumen. Zygotes which were attached to the peritrophic membrane before its penetration were observed 14 – 20 hours post tick repletion. However, in their work, there is no indication whether the zygotes can be present in the tick gut lumen already on the first day of tick feeding since this was never addressed and the authors focused only on parasite stages after tick repletion. According to previous research of Karakashian et al. (1986), kinetes can be found in salivary glands of tick larva 13 days post-repletion. Yet again, the parasite development during tick feeding was never examined. In addition, it is important to highlight that these stages undergo two rounds of multiplication either in different tick tissues and salivary glands or they directly invade salivary glands (Jalovecka et al. 2018). Therefore, the possibility of the parasite's migration and multiplication within 24 hours in the tissue cannot be excluded.

AMA-1 cannot be considered as a universal surface marker of invasive stages of B. microti

In line with a previous study (Moitra et al. 2015), we detected AMA-1 protein in *B. microti* blood stages by indirect immunofluorescence. The method revealed that stages found in the tick gut lumen express AMA-1 protein (Fig. 19; C), unlike the ones which were observed in epithelial cells of tick gut wall (Fig. 19; A, B). Since the gut lumen contains a mixture of ingested asexual as well as developing sexual stages, we assume, we immune-detected ingested merozoites. Although it is important to point out that we cannot exclude AMA-1 protein expression on the sexual stages presented in the tick gut lumen. To the contrary, in tick gut cells only the zygote and kinetes are supposed to be present. Since we did not detect any signal, we assume that AMA-1 protein is not expressed on the surface of these intra-tick invasive stages.

Based on previous research it is evident that zygote penetrates the peritrophic membrane using a special organ known as arrowhead (Rudzinska et al. 1982). Kinetes which develop from the zygote lack this organ and possess organelles of apical complex instead (Karakashian et al. 1986). However, a single large rhoptry, which can be found in invasive stages such as sporozoites and merozoites, is missing in kinetes (Karakashian et al. 1986). We hypothesize that since AMA-1 protein interacts with RON2 protein secreted from rhoptries (Bargieri et al. 2014) when the parasite invades cell of the vertebrate host, complex between the proteins cannot be established in the tick. Therefore, expression of AMA-1 protein could be redundant. Although it is worth considering that kinetes can express the gene but not the protein itself which would be supported by *ama-1* expression in salivary glands. Up to now, no solid evidence on the mechanism and the proteins used by kinetes for the invasion of tick tissues has been provided. It is possible that these stages enter the tissues using a combination of different proteins which would be worth studying in the future.

Unfortunately, in this work, we were not able to present the proof of AMA-1 expression in mature sporozoites in salivary glands although we detected *ama-1* gene expression in early stages of parasite development in tick salivary glands (Fig. 14). Since the microscopy analysis of a single tissue is time-demanding, so far we have not observed samples thoroughly to obtain representative results. As mature sporozoites acquire secretory organelles the presence of AMA-1 protein cannot be ruled out (Karakashian et al. 1983). Whether AMA-1 can be used as a surface marker of mature sporozoites in salivary glands is therefore yet to be elucidated. To sum up the results of immunodetection, we verified that AMA-1 protein cannot be used for identification of asexual stages (kinetes) in the tick gut epithelial cells.

AMA-1 is involved in the host immune response

Infection with *B. microti* was already confirmed to be self-limiting in BALB/c mice (Igarashi et al. 1999). The ability to recover from the infection makes BALB/c mice a convenient model for studying the dynamics of the immune response towards *B. microti*. Since we did not observe the parasite on the blood smears even 30 days post-infection, we assumed that the mice recovered from the acute infection. However, using nested PCR, we found out that the parasite was still present in the blood of mice (Fig. 10; B). Parasitemia was maintained at very low levels and hence under the detection limit of microscopical examination.

Results from re-infection challenge studies demonstrated the development of protective immunity in BALB/c mice (Fig. 20). The first infection with *B. microti* prevented the progress of acute infection in mice which were later challenged in different intervals (up to 90 days) post the first infection. Subsequently, we examined whether the mice could develop a humoral immune response against AMA-1 since the protein has been tested as one of the candidates involved in anti-malarial vaccine before (Remarque et al. 2008). Moreover, in several studies, AMA-1 has been proven as a crucial target for reducing the growth of the parasite *in vitro* (Montero et al. 2009; Moitra et al. 2015). We confirmed that the majority of mice generated antibodies against AMA-1 recombinant protein (Fig. 21). Therefore, we can conclude that AMA-1 is involved in host immune response.

However, the protective/memory immunity is very likely generated as a response to multiple parasite antigens expressed on parasite blood stages. For example, Wang et al (2017) stated that rather than the total amount of generated antibodies against single antigens of *B. microti* such as AMA-1 and RON2, the presence of antibodies which target the epitopes of AMA-1 and RON2 in combination is more crucial for effective immune response. Therefore, it is presumable that the other surface proteins of parasite blood stages will contribute to the fully protective immunity apparent from our re-infection experiment (Fig. 20). Nevertheless, the potential protective role of AMA-1 protein still needs to be verified by immunization of mice with recombinant AMA-1 protein and subsequent *B. microti* challenge.

CCp2 as a potential surface marker of B. microti sexual stages within the tick host

The sexual commitment of the parasite starts already in the vertebrate host. The gametocytes were found to completely reorganize the cytoplasm and the structures within once they enter the tick gut lumen (Rudzinska et al. 1979). Newly emerged gametes possess an arrowhead structure. Currently, it is not known whether the arrowhead is a modification of the apical complex and whether the gametes also express AMA-1. Although the study with *Eimeria* indicated that AMA-1 is gametocyte specific (Jiang et al. 2012). This could potentially be an explanation of *ama-1* expression in the gut on the 6th day after tick repletion. Thus, we focused on CCp2 protein which has been previously studied as a specific surface-associated protein of apicomplexan sexual stages (Becker et al. 2010; Bastos et al. 2013).

Expression of *ccp2* gene fluctuated in the host blood (fig. 22). It is possible that the expression pattern correlates with the fluctuating commitment to gametocytogenesis and emergence of new gametocytes. Bastos et al. (2013) previously confirmed facultative expression of *ccp* genes in *B. bovis* and *Theileria equi in vivo*. *Ccp* genes of *T. equi* manifested two waves of expression which corresponds with our results. Also, Jalovecka et al. (2016) have shown that levels of gametocytes fluctuate during *B. divergens* culture *in vitro*. Expression of *ccp2* in the tick gut presumably indicates the presence of sexual stages in the lumen. The expression stayed elevated even six days post-repletion which probably means that sexual stages still persist in there (Fig. 23).

Expression of *ccp2* was detected also in salivary glands where the future sporozoites will evolve (Fig. 24). Correspondingly, CCp2 was found in the proteome of sporozoites of *C. parvum* (citace). However, it is difficult to speculate on possible roles of CCp2 in the asexual reproduction of the parasite in the salivary glands. The gene can be transcribed for the future developmental stages but does not have to be translated into the protein. In the future, we intend to localize CCp2 protein in sexual stages in the tick gut lumen and examine also the parasites in salivary glands. CCp2 recombinant protein has been already synthesized and currently, we are in the phase of rabbit immunization.

6. Conclusion

AMA-1 has been previously described as a protein associated with the apical complex and involved in the process of host cell invasion (Bargieri et al. 2014). Since apical organelles secreting AMA-1 can be found also in invasive intra-tick stages (Karakashian et al. 1986), the protein has been selected for further examination and also for immuno-detection of *B. microti* within the tick host. In accordance with previous concept, the expression of AMA-1 was validated in *B. microti* blood stages. Moreover, the protein was proven to generate a humoral immune response in the vertebrate host. In the tick internal organs – gut and salivary glands – the expression of *ama-1* gene was detected. Yet, no protein expression was detected in kinetes in the gut wall unlike in the stages in the gut lumen.

CCp2 protein, which has been formerly identified as a sexual stage-specific marker in another *Babesia* species (Becker et al. 2013), was intended to be used for distinguishing sexual and asexual stages of *B. microti* in the gut lumen. The *ccp2* gene expression was confirmed also in the tick tissues indicating the presence of the sexual stages in the gut lumen. In the future, using both anti-AMA-1 and anti-CCp2 antibodies would elucidate representation of the single stages in the tick gut.

Overall, the results demonstrated that AMA-1 protein cannot be used as a marker for the identification of *B. microti* asexual stages (kinetes) in the tick gut epithelial cells. Therefore, future research will be conducted on the examination of other potential surface markers. CCp2 protein appears to be a promising surface marker of sexual stages and will be further investigated.

7. References

- Alkische, A. A., et al. (2017). "Climate change influences on the potential geographic distribution of the disease vector tick *Ixodes ricinus*." PLoS one 12(12): e0189092.
- Baneth, G., et al. (2015). "Reclassification of *Theileria annae* as *Babesia vulpes* sp. nov." Parasites & vectors 8(1): 207.
- Bannister, L. H., et al. (2003). "*Plasmodium falciparum* apical membrane antigen 1 (PfAMA-1) is translocated within micronemes along subpellicular microtubules during merozoite development." Journal of cell science 116(18): 3825-3834.
- Bargieri, D., et al. (2014). "Host cell invasion by apicomplexan parasites: the junction conundrum." PLoS pathogens 10(9): e1004273.
- Bargieri, D. Y., et al. (2013). "Apical membrane antigen 1 mediates apicomplexan parasite attachment but is dispensable for host cell invasion." Nature communications 4: 2552.
- Bastos, R. G., et al. (2013). "Differential expression of three members of the multidomain adhesion CCp family in *Babesia bigemina*, *Babesia bovis* and *Theileria equi*." PLoS one 8(7): e67765.
- Beck, R., et al. (2011). "Molecular survey of *Babesia microti* in wild rodents in central Croatia." Vector Borne Zoonotic Dis 11(1): 81-83.
- Becker, C., et al. (2010). "Identification of three CCp genes in *Babesia* : novel markers for sexual stages parasites." Molecular and biochemical parasitology 174(1): 36-43.
- Becker, C. A., et al. (2013). "Validation of BdCCp2 as a marker for *Babesia divergens* sexual stages in ticks." Experimental parasitology 133(1): 51-56.
- Besteiro, S., et al. (2011). "The moving junction of apicomplexan parasites: a key structure for invasion." Cellular microbiology 13(6): 797-805.
- Besteiro, S., et al. (2009). "Export of a *Toxoplasma gondii* rhoptry neck protein complex at the host cell membrane to form the moving junction during invasion." PLoS pathogens 5(2): e1000309.
- Birkenheuer, A. J., et al. (2005). "Geographic distribution of babesiosis among dogs in the United States and association with dog bites: 150 cases (2000–2003)." Journal of the American Veterinary Medical Association 227(6): 942-947.
- Bock, R., et al. (2004). "Babesiosis of cattle." Parasitology 129 Suppl: S247-269.
- Centeno-Lima, S., et al. (2003). "A fatal case of human babesiosis in Portugal: molecular and phylogenetic analysis." Trop Med Int Health 8(8): 760-764.
- Collins, C. R., et al. (2009). "An inhibitory antibody blocks interactions between components of the malarial invasion machinery." PLoS pathogens 5(1): e1000273.
- Crawford, J., et al. (2010). "Structural characterization of apical membrane antigen 1 (AMA1) from *Toxoplasma gondii*." Journal of Biological Chemistry 285(20): 15644-15652.
- Dammin, G. J., et al. (1981). "The rising incidence of clinical *Babesia microti* infection." Human pathology 12(5): 398-400.
- de Waal, D. T. and M. P. Combrink (2006). "Live vaccines against bovine babesiosis." Vet Parasitol 138(1-2): 88-96.
- Dessens, J. T., et al. (2004). "LCCL proteins of apicomplexan parasites." Trends in parasitology 20(3): 102-108.
- Donahue, C. G., et al. (2000). "The *Toxoplasma* homolog of *Plasmodium* apical membrane antigen-1 (AMA-1) is a microneme protein secreted in response to elevated intracellular calcium levels." Molecular and biochemical parasitology 111(1): 15-30.
- Duh, D., et al. (2001). "Diversity of *Babesia* Infecting European sheep ticks (*Ixodes ricinus*)." J Clin Microbiol 39(9): 3395-3397.
- Duh, D., et al. (2003). "The molecular evidence of *Babesia microti* infection in small mammals collected in Slovenia." Parasitology 126(2): 113-117.
- Etkind, P., et al. (1980). "Methods for detecting *Babesia microti* infection in wild rodents." The Journal of parasitology 66(1): 107-110.
- Foppa, I. M., et al. (2002). "Entomologic and serologic evidence of zoonotic transmission of *Babesia microti*, eastern Switzerland." Emerg Infect Dis 8(7): 722-726.
- Gaffar, F. R., et al. (2004). "Erythrocyte invasion by *Babesia bovis* merozoites is inhibited by polyclonal antisera directed against peptides derived from a homologue of *Plasmodium falciparum* apical membrane antigen 1." Infection and immunity 72(5): 2947-2955.

- Giovannini, D., et al. (2011). "Independent roles of apical membrane antigen 1 and rhoptry neck proteins during host cell invasion by apicomplexa." *Cell host & microbe* 10(6): 591-602.
- Gohil, S., et al. (2013). "Bovine babesiosis in the 21st century: advances in biology and functional genomics." *Int J Parasitol* 43(2): 125-132.
- Gohil, S., et al. (2010). "Recent insights into alteration of red blood cells by *Babesia bovis*: moovin'forward." *Trends in parasitology* 26(12): 591-599.
- Gray, J., et al. (2002). "Transmission studies of *Babesia microti* in *Ixodes ricinus* ticks and gerbils." *Journal of Clinical Microbiology* 40(4): 1259-1263.
- Gray, J., et al. (2010). "Zoonotic babesiosis: overview of the disease and novel aspects of pathogen identity." *Ticks and tick-borne diseases* 1(1): 3-10.
- Haapasalo, K., et al. (2010). "Fatal babesiosis in man, Finland, 2004." *Emerg Infect Dis* 16(7): 1116-1118.
- Haselbarth, K., et al. (2007). "First case of human babesiosis in Germany - Clinical presentation and molecular characterisation of the pathogen." *Int J Med Microbiol* 297(3): 197-204.
- Hehl, A. B., et al. (2000). "*Toxoplasma gondii* Homologue of *Plasmodium* Apical Membrane Antigen 1 Is Involved in Invasion of Host Cells." *Infection and immunity* 68(12): 7078-7086.
- Hersh, M. H., et al. (2012). "Reservoir competence of wildlife host species for *Babesia microti*." *Emerging infectious diseases* 18(12): 1951.
- Herwaldt, B. L., et al. (2003). "Molecular characterization of a non-*Babesia* divergens organism causing zoonotic babesiosis in Europe." *Emerg Infect Dis* 9(8): 942-948.
- Hildebrandt, A., et al. (2013). "Human babesiosis in Europe: what clinicians need to know." *Infection* 41(6): 1057-1072.
- Hodder, A. N., et al. (1996). "The disulfide bond structure of *Plasmodium* apical membrane antigen-1." *Journal of Biological Chemistry* 271(46): 29446-29452.
- Homer, M. J., et al. (2000). "Babesiosis." *Clin Microbiol Rev* 13(3): 451-469. facilitating diagnosis, expediting appropriate patient management, and resulting in a more accurate epidemiological description.
- Igarashi, I., et al. (1999). "Roles of CD4+ T Cells and Gamma Interferon in Protective Immunity against *Babesia microti* Infection in Mice." *Infection and immunity* 67(8): 4143-4148.
- Irwin, P. J. (2009). "Canine babesiosis: from molecular taxonomy to control." *Parasit Vectors* 2 Suppl 1: S4.
- Jalovecka, M., et al. (2016). "Stimulation and quantification of *Babesia divergens* gametocytogenesis." *Parasites & vectors* 9(1): 439.
- Jalovecka, M. (2017). "Establishment of *Babesia* laboratory model and its experimental application." Ph.D. Thesis, in English – 180 pp., Doctoral School of Biology and Health, University of Bretagne-Loire, Nantes-Atlantic College of Veterinary Medicine and Food Sciences and Engineering, Nantes, France.
- Jalovecka, M., et al. (2018). "The complexity of piroplasms life cycles." *Frontiers in cellular and infection microbiology* 8: 248.
- Jalovecka, M., et al. (2019). "*Babesia* Life Cycle—When Phylogeny Meets Biology." *Trends in parasitology*.
- Jefferies, R., et al. (2007). "Blood, bull terriers and babesiosis: further evidence for direct transmission of *Babesia gibsoni* in dogs." *Australian veterinary journal* 85(11): 459-463.
- Jiang, L., et al. (2012). "Identification and characterization of *Eimeria tenella* apical membrane antigen-1 (AMA1)." *PloS one* 7(7): e41115.
- Karakashian, S. J., et al. (1986). "Primary and secondary ookinetes of *Babesia microti* in the larval and nymphal stages of the tick *Ixodes dammini*." *Canadian journal of zoology* 64(2): 328-339.
- Karakashian, S. J., et al. (1983). "Ultrastructural studies on sporogony of *Babesia microti* in salivary gland cells of the tick *Ixodes dammini*." *Cell and tissue research* 231(2): 275-287.
- Kim, J. Y., et al. (2007). "First case of human babesiosis in Korea: detection and characterization of a novel type of *Babesia* sp. (KO1) similar to ovine babesia." *J Clin Microbiol* 45(6): 2084-2087.
- Krause, P. J., et al. (2000). "Atovaquone and azithromycin for the treatment of babesiosis." *New England Journal of Medicine* 343(20): 1454-1458.
- Kuehn, A., et al. (2010). "Family members stick together: multi-protein complexes of malaria parasites." *Med Microbiol Immunol* 199(3): 209-226.
- Lamarque, M., et al. (2011). "The RON2-AMA1 interaction is a critical step in moving junction-dependent invasion by apicomplexan parasites." *PLoS pathogens* 7(2): e1001276.

- Lasonder, E., et al. (2002). "Analysis of the *Plasmodium falciparum* proteome by high-accuracy mass spectrometry." *Nature* 419(6906): 537-542.
- Leiby, D. A. (2011). "Transfusion-associated babesiosis: shouldn't we be ticked off?" *Annals of internal medicine* 155(8): 556-557.
- Malandrin, L., et al. (2010). "Redescription of *Babesia capreoli* (Enigk and Friedhoff, 1962) from roe deer (*Capreolus capreolus*): isolation, cultivation, host specificity, molecular characterisation and differentiation from *Babesia divergens*." *International journal for parasitology* 40(3): 277-284.
- Mehlhorn, H. and E. Schein (1993). "The piroplasms: "A long story in short" or "Robert Koch has seen it"." *Eur J Protistol* 29(3): 279-293.
- Mital, J., et al. (2005). "Conditional expression of *Toxoplasma gondii* apical membrane antigen-1 (TgAMA1) demonstrates that TgAMA1 plays a critical role in host cell invasion." *Molecular biology of the cell* 16(9): 4341-4349.
- Moitra, P., et al. (2015). "Expression, Purification, and Biological Characterization of *Babesia microti* Apical Membrane Antigen 1." *Infect Immun* 83(10): 3890-3901.
- Montero, E., et al. (2009). "*Babesia divergens* apical membrane antigen 1 and its interaction with the human red blood cell." *Infection and immunity* 77(11): 4783-4793.
- Morrisette, N. S. and L. D. Sibley (2002). "Cytoskeleton of apicomplexan parasites." *Microbiol Mol Biol Rev* 66(1): 21-38; table of contents.
- Oyamada, M., et al. (2005). "Detection of *Babesia canis rossi*, *B. canis vogeli*, and *Hepatozoon canis* in dogs in a village of eastern Sudan by using a screening PCR and sequencing methodologies." *Clin. Diagn. Lab. Immunol.* 12(11): 1343-1346.
- Pfaffl, M. W. (2001). "A new mathematical model for relative quantification in real-time RT-PCR." *Nucleic acids research* 29(9): e45-e45.
- Pizarro, J. C., et al. (2005). "Crystal structure of the malaria vaccine candidate apical membrane antigen 1." *Science* 308(5720): 408-411.
- Poukchanski, A., et al. (2013). "*Toxoplasma gondii* sporozoites invade host cells using two novel paralogues of RON2 and AMA1." *PloS one* 8(8): e70637.
- Pradel, G., et al. (2004). "A multi-domain adhesion protein family expressed in *Plasmodium falciparum* gametocytes is essential for sporozoite midgut to salivary gland transition." *International Journal of Medical Microbiology* 293: 97.
- Rar, V. A., et al. (2011). "Genetic diversity of *Babesia* in *Ixodes persulcatus* and small mammals from North Ural and West Siberia, Russia." *Parasitology* 138(2): 175-182.
- Remarque, E. J., et al. (2008). "Apical membrane antigen 1: a malaria vaccine candidate in review." *Trends in parasitology* 24(2): 74-84.
- Richard, D., et al. (2010). "Interaction between *Plasmodium falciparum* apical membrane antigen 1 and the rhoptry neck protein complex defines a key step in the erythrocyte invasion process of malaria parasites." *Journal of Biological Chemistry* 285(19): 14815-14822.
- Rudzinska, M., et al. (1984). The sequence of developmental events of *Babesia microti* in the gut of *Ixodes dammini* *Protistologica*. 4: 649-663.
- Rudzinska, M. A., et al. (1982). "Penetration of the peritrophic membrane of the tick by *Babesia microti*." *Cell Tissue Res* 221(3): 471-481.
- Rudzinska, M. A., et al. (1983). "Sexuality in piroplasms as revealed by electron microscopy in *Babesia microti*." *Proc Natl Acad Sci U S A* 80(10): 2966-2970.
- Rudzinska, M. A., et al. (1979). "Intraerythrocytic 'gametocytes' of *Babesia microti* and their maturation in ticks." *Can J Zool* 57(2): 424-434.
- Rudzinska, M. A. and W. Trager (1977). "Formation of merozoites in intraerythrocytic *Babesia microti*: an ultrastructural study." *Canadian journal of zoology* 55(6): 928-938.
- Rudzinska, M. A., et al. (1976). "An electron microscopic study of *Babesia microti* invading erythrocytes." *Cell and tissue research* 169(3): 323-334.
- Sebek, Z., et al. (1977). "The occurrence of babesiosis affecting small terrestrial mammals and the importance of this zoonosis in Europe." *Folia parasitologica* 24(3): 221-228.
- Senanayake, S. N., et al. (2012). "First report of human babesiosis in Australia." *Med J Aust* 196(5): 350-352.
- Shih, C. M., et al. (1997). "Human babesiosis in Taiwan: asymptomatic infection with a *Babesia microti*-like organism in a Taiwanese woman." *J Clin Microbiol* 35(2): 450-454.

- Silvie, O., et al. (2004). "A role for apical membrane antigen 1 during invasion of hepatocytes by *Plasmodium falciparum* sporozoites." *Journal of Biological Chemistry* 279(10): 9490-9496.
- Skrabalo, Z. and Z. Deanovic (1957). "Piroplasmosis in Man. Report on a Case." *Documenta de medicina geographica et tropica* 9(1): 11-16.
- Snelling, W. J., et al. (2007). "Proteomics analysis and protein expression during sporozoite excystation of *Cryptosporidium parvum* (Coccidia, Apicomplexa)." *Mol Cell Proteomics* 6(2): 346-355.
- Solano-Gallego, L. and G. Baneth (2011). "Babesiosis in dogs and cats—expanding parasitological and clinical spectra." *Veterinary parasitology* 181(1): 48-60.
- Sonenshine, D. E. and R. M. Roe. (2014). *Biology of ticks*. New York: Oxford University Press, 2014. ISBN 0199744068.
- Suarez, C. E., et al. (2019). "Unravelling the cellular and molecular pathogenesis of bovine babesiosis: is the sky the limit?" *International journal for parasitology*.
- Tosini, F., et al. (2004). "A new modular protein of *Cryptosporidium parvum*, with ricin B and LCCL domains, expressed in the sporozoite invasive stage." *Mol Biochem Parasitol* 134(1): 137-147.
- Tosini, F., et al. (2006). "Apicomplexa genes involved in the host cell invasion: the Cpa135 protein family." *Parassitologia* 48(1-2): 105-107.
- Trexler, M., et al. (2000). "The LCCL module." *Eur J Biochem* 267(18): 5751-5757.
- Triglia, T., et al. (2000). "Apical membrane antigen 1 plays a central role in erythrocyte invasion by *Plasmodium* species." *Molecular microbiology* 38(4): 706-718.
- Tyler, J. S. and J. C. Boothroyd (2011). "The C-terminus of *Toxoplasma* RON2 provides the crucial link between AMA1 and the host-associated invasion complex." *PLoS pathogens* 7(2): e1001282.
- Tyler, J. S., et al. (2011). "Focus on the ringleader: the role of AMA1 in apicomplexan invasion and replication." *Trends in parasitology* 27(9): 410-420.
- Vannier, E. G., et al. (2015). "Babesiosis." *Infect Dis Clin North Am* 29(2): 357-370.
- Votypka, J. et al. (2017). Apicomplexa. In *Handbook of the Protists* (2nd edn) (Archibald, J.M., ed.), pp. 1–58, Springer International Publishing.
- Vulliez-Le Normand, B., et al. (2012). "Structural and functional insights into the malaria parasite moving junction complex." *PLoS pathogens* 8(6): e1002755.
- Wang, G., et al. (2017). "Expression of truncated *Babesia microti* apical membrane protein 1 and rhoptry neck protein 2 and evaluation of their protective efficacy." *Experimental parasitology* 172: 5-11.
- Wei, Q., et al. (2001). "Human babesiosis in Japan: isolation of *Babesia microti*-like parasites from an asymptomatic transfusion donor and from a rodent from an area where babesiosis is endemic." *J Clin Microbiol* 39(6): 2178-2183.
- Welc-Faleciak, R., et al. (2010). "Co-infection with *Borrelia* species and other tick-borne pathogens in humans: two cases from Poland." *Ann Agric Environ Med* 17(2): 309-313.
- Welc-Faleciak, R., et al. (2015). "First report of two asymptomatic cases of human infection with *Babesia microti* (Franca, 1910) in Poland." *Annals of Agricultural and Environmental Medicine* 22(1).
- Wormser, G. P., et al. (2006). "The clinical assessment, treatment, and prevention of Lyme disease, human granulocytic anaplasmosis, and babesiosis: clinical practice guidelines by the Infectious Diseases Society of America." *Clinical Infectious Diseases* 43(9): 1089-1134.
- Yabsley, M. J. and B. C. Shock (2013). "Natural history of zoonotic *Babesia*: role of wildlife reservoirs." *International Journal for Parasitology: Parasites and Wildlife* 2: 18-31.
- Zamoto-Niikura, A., et al. (2016). "*Ixodes persulcatus* ticks as vectors for the *Babesia microti* US lineage in Japan." *Appl. Environ. Microbiol.* 82(22): 6624-6632.
- Zintl, A., et al. (2003). "*Babesia divergens*, a bovine blood parasite of veterinary and zoonotic importance." *Clinical microbiology reviews* 16(4): 622-636.

Centers for Disease Control and Prevention. National Notifiable Diseases Surveillance System, 2017 Annual Tables of Infectious Disease Data. Atlanta, GA. CDC Division of Health Informatics and Surveillance, 2018.

U.S. Department of Health and Human Services. Food and Drug Administration. Center for Biologics Evaluation and Research. Recommendations for Reducing the Risk of Transfusion-Transmitted Babesiosis, 2018.